Wessex Archaeology

Seabed Prehistory: Site Evaluation Techniques (Area 240)

Synthesis: Appendices

Final Report

Ref: 70754.04

March 2011

SEABED PREHISTORY:
SITE EVALUATION TECHNIQUES (AREA 240)

SYNTHESIS

APPENDICES

FINAL REPORT

Prepared by:

Wessex Archaeology
Portway House
Old Sarum Park
Salisbury
WILTSHIRE
SP4 6EB

Prepared for:

English Heritage

March 2011

Ref: 70754.04

APPENDIX I: RADIOCARBON DATING

John Meadows
1 Waterhouse Square
138-142 Holborn
London EC1N 2ST
020 7973 3273
john.meadows@english-heritage.org.uk

3rd December 2010

Seabed Prehistory Area 240: radiocarbon dating for 70754 VC8c1

Vibrocore VC8c1 sampled a broad and shallow north-east to south-west palaeogeographic feature known as channel B, situated in the north-western corner of the survey area and part of a southerly flowing, meandering channel, in c.30m of water, approximately 11km off the coast of Great Yarmouth. It is thought to have been infilled during the early Holocene.

Four samples of horizontally bedded *Phragmites* reeds, at 31.58, 31.69, 31.96 and 32.00m below OD, were taken from an organic sediment unit, "unit 7" from within vibrocore VC8c1. Each sample consisted of a single waterlogged plant macrofossil, identified by Dr Chris Stevens of Wessex Archaeology. The samples were submitted for Accelerator Mass Spectrometry (AMS) radiocarbon dating to the Oxford Radiocarbon Accelerator Unit at Oxford University and the Scottish Universities Environmental Research Centre in East Kilbride.

Unfortunately both of the samples sent to Oxford failed, due to low yields (Brock *et al* 2010 describe relevant pretreatments). The samples sent to SUERC were successfully dated, however, following technical procedures described by Vandenputte *et al.* (1996), Slota *et al.* (1987), and Xu *et al.* (2004). Internal quality assurance procedures and international inter-comparisons (Scott 2003) indicate no laboratory offsets, and validate the measurement precision given. Laboratory certificates for all four samples are enclosed for the project archive.

The BP results reported in Table 1 are conventional radiocarbon ages (Stuiver and Polach 1977), quoted according to the format known as the Trondheim convention (Stuiver and Kra 1986). Their calibrated date ranges have been calculated by the maximum intercept method (Stuiver and Reimer 1986), using the program OxCal v4.1 (Bronk Ramsey 1995; 1998; 2001; 2009) and the IntCal09 data set (Reimer *et al.* 2009), and are quoted in the form recommended by Mook (1986), rounded outwards to decadal endpoints. Figure 1 shows the calibration of these results by the probability method (Stuiver and Reimer 1993), again using OxCal 4.1 and the IntCal09 calibration data. The probability that a sample dates to a particular calendar date corresponds to the height of its probability distribution at that date.

Laboratory code	Sample	Identification	$\delta^{13}C$ (‰)	Radiocarbon age (BP)	Calibrated date range (95% confidence)
SUERC-32233	31.58m bOD	*Phragmites* sp.	-26.5	7820 ±30	6730–6590 cal BC
P28317	31.69m bOD	*Phragmites* sp.	-	failed	-
P28318	31.96m bOD	*Phragmites* sp.	-	failed	-
SUERC-32234	32.00m bOD	*Phragmites* sp.	-25.0	8595 ±35	7710–7560 cal BC

Table 1: radiocarbon results, Seabed Prehistory Area 240, VC8c1

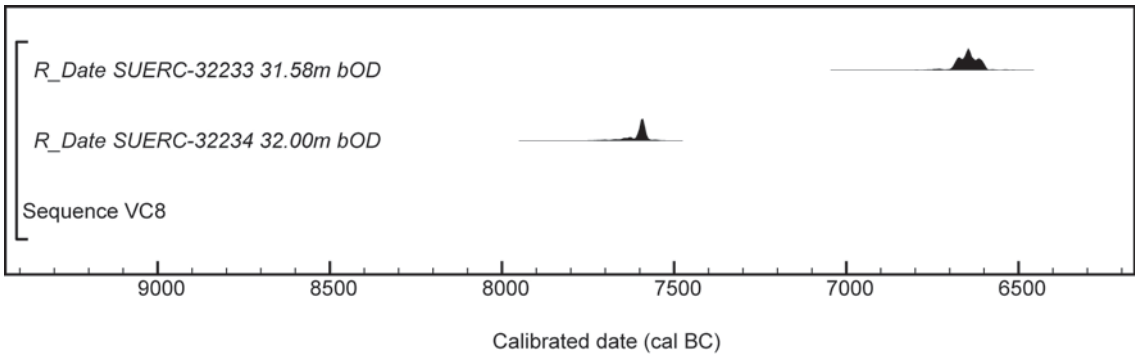

Figure 1. Calibration of the VC8c1 radiocarbon results by the probability method (Stuiver and Reimer 1993), using the IntCal09 calibration data (Reimer *et al*. 2009)

The two samples are clearly different in date, and their date order respects the depositional sequence, so you might reasonably assume that the results provide reliable dates for sedimentation at the corresponding depths in the core. It is a pity that neither of the samples from intermediate levels dated, as it is not difficult to imagine a scenario in which a pair of samples from a disturbed deposit happened to give dates which are apparently in sequence. Nevertheless, at face value the results confirm the interpretation that this channel fill was deposited in the early Holocene.

References

Brock, F., Higham, T., Ditchfield, P., and Bronk Ramsey, C., 2010. Current pretreatment methods for AMS radiocarbon dating at the Oxford Radiocarbon Accelerator Unit (ORAU) *Radiocarbon*, **52**(1), 103–12

Bronk Ramsey, C., 1995. Radiocarbon calibration and analysis of stratigraphy, *Radiocarbon*, **36**, 425–30

Bronk Ramsey, C., 1998. Probability and dating, *Radiocarbon*, **40**, 461–74

Bronk Ramsey, C., 2001. Development of the radiocarbon calibration program, *Radiocarbon*, **43**, 355-63

Bronk Ramsey, C., 2009. Bayesian analysis of radiocarbon dates, *Radiocarbon*, **51**: 337–60

Mook, W. G., 1986. Business meeting: recommendations/resolutions adopted by the twelfth International Radiocarbon Conference, *Radiocarbon*, **28**, 799

Reimer, P. J., Baillie, M.G.L., Bard, E., Bayliss, A., Beck, J.W., Blackwell, P.G., Bronk Ramsey, C., Buck, C.E., Burr, G.S., Edwards, R.L., Friedrich, M., Grootes, P.M., Guilderson, T.P., Hajdas, I., Heaton, T.J., Hogg, A.G., Hughen, K.A., Kaiser, K.F., Kromer, B., McCormac, G., Manning, S., Reimer, R.W., Remmele, S., Richards, D.A., Southon, J.R., Talamo, S., Taylor, F.W., Turney, C.S M., van der Plicht, J., and Weyhenmeyer, C.E., 2009, INTCAL09 and MARINE09 radiocarbon age calibration curves, 0–50,000 years cal BP, *Radiocarbon*, **51**(4), 1111–50

Scott, E.M., 2003. The third international radiocarbon intercomparison (TIRI) and the fourth international radiocarbon intercomparison (FIRI) 1990–2002: results, analyses, and conclusions, *Radiocarbon*, **45**, 135–408

Slota Jr, P.J., Jull, A.J.T., Linick, T.W., and Toolin, L.J., 1987 Preparation of small samples for ^{14}C accelerator targets by catalytic reduction of CO, *Radiocarbon*, **29**, 303–6

Stuiver, M., and Kra, R.S., 1986 Editorial comment, *Radiocarbon*, **28(2B)**, ii

Stuiver, M., and Reimer, P.J., 1986 A computer program for radiocarbon age calculation, *Radiocarbon*, **28**, 1022–30

Stuiver, M., and Reimer, P.J., 1993. Extended ^{14}C data base and revised CALIB 3.0 ^{14}C age calibration program, *Radiocarbon*, **35**, 215–30

Stuiver, M., and Polach, H.A., 1977. Reporting of ^{14}C data, *Radiocarbon*, **19**, 355–63

Vandeputte, K., Moens, L., and Dams, R., 1996. Improved sealed-tube combustion of organic samples to CO_2 for stable isotope analysis, radiocarbon dating and percent carbon determinations, *Analytical Letters*, **29**(15), 2761–73

Xu, S., Anderson, R., Bryant, C., Cook, G.T., Dougans, A., Freeman, S., Naysmith, P., Schnabel, C., and Scott, E.M., 2004. Capabilities of the new SUERC 5MV AMS facility for ^{14}C dating, *Radiocarbon*, **46**, 59–64

APPENDIX II: OPTICALLY STIMULATED LUMINESCENCE DATING

University of Gloucestershire

Geochronology Laboratories

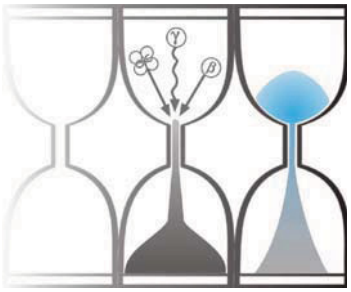

Optical dating of submarine cores: Seabed Prehistory Area 240 Project

to

Wessex Archaeology

Prepared by Dr P.S. Toms, 15 February 2011

Optical dating of submarine cores: Seabed Prehistory Area 240 Project

Dr P.S. Toms

Summary

This study contributes to the Seabed Prehistory Area 240 project, providing Optical age estimates for nine sediment samples obtained from four vibrocores. The time-dependent optically stimulated luminescence signal was calibrated from multi-grain, fine sand aliquots using a single-aliquot, regenerative-dose protocol to provide a measure of natural dose absorption during the burial period. This dosimetry was converted into chronometry by assessing the rate of dose absorption, accounting for litho-cosmogenic emissions along with moisture absorption and grain size attenuation effects. The Optical age estimates generated in this study span from 31 ka (Marine Isotope Stage 2) to greater than 869 ka (Marine Isotope Stage 24). The majority of samples are accompanied by analytical caveats, however all intra-core age estimates are consistent with their relative stratigraphic position. Dose rates are below average for most samples; in such cases age estimates become increasingly sensitive to inaccuracies in D_r as the magnitude of D_r decreases and burial period increases. The reliability of the optical chronology should be measured against any extrinsic temporal control that may be available to the project. If units dated in this study can be shown to be stratigraphically equivalent between cores then it may be possible to assess reliability intrinsically, quantifying the convergence of age estimates from divergent D_r values.

Author's address

Geochronology Laboratories, Department of Natural and Social Sciences, University of Gloucestershire, Swindon Road, Cheltenham. GL50 4AZ. Tel: 01242 544091. Email: ptoms@glos.ac.uk.

1.0 Introduction

This study contributes to the Seabed Prehistory project in Area 240, coordinated by Wessex Archaeology. Sediment cores were retrieved from the North Sea, approximately 11km due east of Great Yarmouth. Elements of four cores (VC2b, VC3b, VC7b and VC9b) were submitted for Optical dating.

2.0 Mechanisms and principles

Upon exposure to ionising radiation, electrons within the crystal lattice of insulating minerals are displaced from their atomic orbits. Whilst this dislocation is momentary for most electrons, a portion of charge is redistributed to meta-stable sites (traps) within the crystal lattice. In the absence of significant optical and thermal stimuli, this charge can be stored for extensive periods. The quantity of charge relocation and storage relates to the magnitude and period of irradiation. When the lattice is optically or thermally stimulated, charge is evicted from traps and may return to a vacant orbit position (hole). Upon recombination with a hole, an electron's energy can be dissipated in the form of light generating crystal luminescence providing a measure of dose absorption.

Herein, quartz is segregated for dating. The utility of this minerogenic dosimeter lies in the stability of its datable signal over the mid to late Quaternary period, predicted through isothermal decay studies (e.g. Smith *et al*., 1990; retention lifetime 630 Ma at 20°C) and evidenced by optical age estimates concordant with independent chronological controls (e.g. Murray and Olley, 2002). This stability is in contrast to the anomalous fading of comparable signals commonly observed for other ubiquitous sedimentary minerals such as feldspar and zircon (Wintle, 1973; Templer, 1985; Spooner, 1993)

Optical age estimates of sedimentation (Huntley *et al*., 1985) are premised upon reduction of the minerogenic time dependent signal (Optically Stimulated Luminescence, OSL) to zero through exposure to sunlight and, once buried, signal reformulation by absorption of litho- and cosmogenic radiation. The signal accumulated post burial acts as a dosimeter recording total dose absorption, converting to a chronometer by estimating the rate of dose absorption quantified through the assay of radioactivity in the surrounding lithology and streaming from the cosmos.

$$\text{Age} = \frac{\text{Mean Equivalent Dose } (D_e, \text{ Gy})}{\text{Mean Dose Rate } (D_r, \text{ Gy.ka}^{-1})}$$

Aitken (1998) and Bøtter-Jensen et al. (2003) offer a detailed review of optical dating.

3.0 Sample Preparation

A total of nine sediment samples were submitted from four vibrocores for Optical dating (Table 1, Image 1). The cores were bisected in daylight to identify the apposite sampling position in consultation with J. Russell, Wessex Archaeology to meet the requirements of the client. To preclude optical erosion of the datable signal prior to measurement both lengths of each core were moved into and prepared under controlled laboratory illumination, provided by Encapsulite RB-10 (red) filters. Sediment exposed to daylight during bisection was removed from each sample position to a depth of 10 mm from each bisected face. The remaining sediment was then sectioned into a 100 mm length, 40 mm wide sample using aluminium separators to preclude incorporation of material transferred down the core walls during submarine retrieval. In the case of sample GL10042, a length of 150 mm was extracted in order to attain sufficient fine sand in the predominantly coarse sand matrix. Sub-samples of c. 50 g were taken from within each position to establish β D_r values and, where feasible, further samples beyond each sample position to estimate γ D_r values.

Each dating sample was then weighed, dried, reweighed and sieved. Quartz within the fine sand (125-180, 180-250 μm) fraction was segregated (Table 1). The samples were then subjected to acid and alkaline digestion (10% HCl, 15% H_2O_2) to attain removal of carbonate and organic components respectively. A further acid digestion in HF (40%, 60 mins) was used to etch the outer 10-15 μm layer affected by α radiation and degrade each samples'

feldspar content. During HF treatment, continuous magnetic stirring was used to effect isotropic etching of grains. 10% HCl was then added to remove acid soluble fluorides. Each sample was dried, resieved and quartz isolated from the remaining heavy mineral fraction using a sodium polytungstate density separation at 2.68g.cm^{-3}. 12 multi-grain aliquots (*c*. 4-6 mg) of quartz from each sample were then mounted on aluminium discs for determination of D_e values.

All drying was conducted at 40°C to prevent thermal erosion of the time-dependent signal. All acids and alkalis were Analar grade. All dilutions (removing toxic-corrosive and non-minerogenic luminescence-bearing substances) were conducted with distilled water to prevent signal contamination by extraneous particles.

4.0 Acquisition and accuracy of D_e value

All minerals naturally exhibit marked inter-sample variability in luminescence per unit dose (sensitivity). Therefore, the estimation of D_e acquired since burial requires calibration of the natural signal using known amounts of laboratory dose. D_e values were quantified using a single-aliquot regenerative-dose (SAR) protocol (Murray and Wintle 2000; 2003) facilitated by a Risø TL-DA-15 irradiation-stimulation-detection system (Markey *et al*., 1997; Bøtter-Jensen *et al*., 1999). Within this apparatus, optical signal stimulation is provided by a 150 W tungsten halogen lamp, filtered to a broad blue-green light, 420-560 nm (2.21-2.95 eV) conveying 16 mWcm^{-2}, using three 2 mm Schott GG420 and a broadband interference filter. Infrared (IR) stimulation, provided by 6 IR diodes (Telefunken TSHA 6203) stimulating at 875±80nm delivering ~5 mW.cm^{-2}, was used to indicate the presence of contaminant feldspars (Hütt *et al*., 1988). Stimulated photon emissions from quartz aliquots are in the ultraviolet (UV) range and were filtered from stimulating photons by 7.5 mm HOYA U-340 glass and detected by an EMI 9235QA photomultiplier fitted with a blue-green sensitive bialkali photocathode. Aliquot irradiation was conducted using a 1.48 GBq ^{90}Sr/^{90}Y β source calibrated for multi-grain aliquots of fine sand sized quartz against the 'Hotspot 800' ^{60}Co γ source located at the National Physical Laboratory (NPL), UK.

SAR by definition evaluates D_e through measuring the natural signal (Fig. 1) of a single aliquot and then regenerating that aliquot's signal by using known laboratory doses to enable calibration. For each aliquot, 5 different regenerative-doses were administered so as to image dose response. D_e values for each aliquot were then interpolated, and associated counting and fitting errors calculated, by way of exponential plus linear regression (Fig. 1). Weighted (geometric) mean D_e values were calculated from 12 aliquots using the central age model outlined by Galbraith *et al*. (1999) and are quoted at 1σ confidence. The accuracy with which D_e equates to total absorbed dose and that dose absorbed since burial was assessed. The former can be considered a function of laboratory factors, the latter, one of environmental issues. Diagnostics were deployed to estimate the influence of these factors and criteria instituted to optimise the accuracy of D_e values.

4.1 Laboratory Factors

4.1.1 Feldspar contamination

The propensity of feldspar signals to fade and underestimate age, coupled with their higher sensitivity relative to quartz makes it imperative to quantify feldspar contamination. At room temperature, feldspars generate a signal (IRSL) upon exposure to IR whereas quartz does not. The signal from feldspars contributing to OSL can be depleted by prior exposure to IR. For all aliquots the contribution of any remaining feldspars was estimated from the OSL IR depletion ratio (Duller, 2003). If the addition to OSL by feldspars is insignificant, then the repeat dose ratio of OSL to post-IR OSL should be statistically consistent with unity (Fig. 1 and Fig. 5). If any aliquots do not fulfil this criterion, as in the case of GL10042 and GL10043, then the sample age estimate should be accepted

tentatively. The source of feldspar contamination is rarely rooted in sample preparation; it predominantly results from the occurrence of feldspars as inclusions within quartz.

4.1.2 Preheating

Preheating aliquots between irradiation and optical stimulation is necessary to ensure comparability between natural and laboratory-induced signals. However, the multiple irradiation and preheating steps that are required to define single-aliquot regenerative-dose response leads to signal sensitisation, rendering calibration of the natural signal inaccurate. The SAR protocol (Murray and Wintle, 2000; 2003) enables this sensitisation to be monitored and corrected using a test dose, here set at 10 Gy preheated to 220°C for 10s, to track signal sensitivity between irradiation-preheat steps. However, the accuracy of sensitisation correction for both natural and laboratory signals can be preheat dependent.

The Dose Recovery test was used to assess the optimal preheat temperature for accurate correction and calibration of the time dependent signal. Dose Recovery (Fig. 2) attempts to quantify the combined effects of thermal transfer and sensitisation on the natural signal, using a precise lab dose to simulate natural dose. The ratio between the applied dose and recovered D_e value should be statistically concordant with unity. For this diagnostic, 6 aliquots were each assigned a 10 s preheat between 180°C and 280°C.

That preheat treatment fulfilling the criterion of accuracy within the Dose Recovery test (Table 1) was selected to generate the final D_e value. Two samples, GL10041 and GL10043, failed to retrieve the applied dose irrespective of preheat treatment; their associated age estimates should therefore be accepted tentatively. Further thermal treatments, prescribed by Murray and Wintle (2000; 2003), were applied to optimise accuracy and precision. Optical stimulation was conducted at 125ºC in order to minimise effects associated with photo-transferred thermoluminescence and maximise signal to noise ratios. Inter-cycle optical stimulation was conducted at 280°C to minimise recuperation.

4.1.3 Irradiation

For all samples having D_e values in excess of 100 Gy, matters of signal saturation and laboratory irradiation effects are of concern. With regards the former, the rate of signal accumulation generally adheres to a saturating exponential form and it is this that limits the precision and accuracy of D_e values for samples having absorbed large doses. For such samples, the functional range of D_e interpolation by SAR has been verified up to 600 Gy by Pawley *et al*. (2010). Age estimates based on D_e values exceeding this value should be accepted tentatively. Whilst no mean D_e value exceeded 600 Gy, 25% of aliquots in GL10040 did with the natural dose proving to be saturated. In this case, the resulting age estimate is considered a minimum value.

4.1.4 Internal consistency

Quasi-radial plots (*cf* Galbraith, 1990) are used to illustrate inter-aliquot D_e variability for natural, repeat regenerative-dose and OSL to post-IR OSL signals (Figs. 3 to 5, respectively). D_e values are standardised relative to the central D_e value for natural signals and applied dose for regenerated signals. D_e values are described as overdispersed when >5% lie beyond $\pm 2\sigma$ of the standardising value; resulting from a heterogeneous absorption of burial dose and/or response to the SAR protocol. For multi-grain aliquots, overdispersion of natural signals does not necessarily imply inaccuracy. However where overdispersion is observed for regenerated signals, as in the case of all but one sample (GL10037) in this study, the resulting age estimate should be accepted tentatively.

4.2 Environmental factors

4.2.1 Incomplete zeroing

Post-burial OSL signals residual of pre-burial dose absorption can result where pre-burial sunlight exposure is limited in spectrum, intensity and/or period, leading to age overestimation. This effect is particularly acute for material eroded and redeposited sub-aqueously (Olley *et al*., 1998, 1999; Wallinga, 2002) and exposed to a burial dose of <20 Gy (e.g. Olley *et al*., 2004). It has some influence in sub-aerial contexts but is rarely of consequence where aerial transport has occurred.

Within single-aliquot regenerative-dose optical dating there are two diagnostics of partial resetting (or bleaching); signal analysis (Agersnap-Larsen *et al*., 2000; Bailey *et al*., 2003) and inter-aliquot D_e distribution studies (Murray *et al*., 1995). Within this study, signal analysis was used to quantify the change in D_e value with respect to optical stimulation time for multi-grain aliquots. This exploits the existence of traps within minerogenic dosimeters that bleach with different efficiency for a given wavelength of light to verify partial bleaching. D_e (t) plots (Fig. 6; Bailey *et al*., 2003) are constructed from separate integrals of signal decay as laboratory optical stimulation progresses. A statistically significant increase in natural D_e (t) is indicative of partial bleaching assuming three conditions are fulfilled. Firstly, that a statistically significant increase in D_e (t) is observed when partial bleaching is simulated within the laboratory. Secondly, that there is no significant rise in D_e (t) when full bleaching is simulated. Finally, there should be no significant augmentation in D_e (t) when zero dose is simulated. Where partial bleaching is detected, as in the case of sample GL10042, the age derived from the sample should be considered a maximum estimate only. However, the utility of signal analysis is strongly dependent upon a samples pre-burial experience of sunlight's spectrum and its residual to post-burial signal ratio. Given in the majority of cases, the spectral exposure history of a deposit is uncertain, the absence of an increase in natural D_e (t) does not necessarily testify to the absence of partial bleaching.

4.2.2 Turbation

The accuracy of sedimentation ages can further be controlled by post-burial trans-strata grain movements forced by pedo- or cryoturbation (e.g. Bateman et al., 2003). Though assumed to reflect former terrestrial sediments, none of the samples showed visible signs of pedogenesis or cryogenic deformation.

5.0 Acquisition and accuracy of D_r value

Lithogenic Dr values were defined through measurement of U, Th and K radionuclide concentration and conversion of these quantities into β and γ Dr values external to the quartz grains (Table 1). External β contributions were estimated from sub-samples by laboratory-based γ spectrometry using an Ortec GEM-S high purity Ge coaxial detector system, calibrated using certified reference materials supplied by CANMET. γ dose rates can be estimated from in situ NaI gamma spectrometry to reduce uncertainty relating to potential heterogeneity in the γ dose field surrounding each sample. Where direct measurements are unavailable as in the present case, laboratory-based Ge γ spectrometry can be used to profile the γ field. Where feasible, sub-samples at intervals within 300 mm above and below of each sample's centre were taken, individually homogenised and then combined in proportion to the γ gradient hypothesised by Løvborg (Aitken, 1985). Estimates of radionuclide concentration were converted into Dr values (Adamiec and Aitken, 1998), accounting for Dr modulation forced by grain size (Mejdahl, 1979) and present moisture content (Zimmerman, 1971). Internal α Dr was assumed to be 0.06±0.03 Gy.ka-1. Cosmogenic Dr values were calculated on the basis of sample depth, geographical position and matrix density (Prescott and Hutton, 1994).

The spatiotemporal validity of Dr values can be considered a function of five variables. Firstly, age estimates devoid of in situ γ spectrometry data or laboratory-based γ profiling should be accepted tentatively; this applies to samples GL10038, GL10040 and GL10043. Secondly, disequilibrium can force temporal instability in U and Th emissions (Olley et al., 1996). Though considered prevalent in surficial marine sediments, owing principally to unsupported U isotopes scavenged from the water column (Jakobsen et al., 2003; Stokes et al., 2003), the assumed terrestrial genus of the deposits should mean that significant disequilibrium is unlikely. However, samples GL10038 and possibly GL10043 show this effect to be pronounced (>50% disequilibrium between 238U and 226Ra; Fig. 7) and thus the resulting age estimates should be accepted tentatively. It may be that U disequilibrium is relatively significant in other samples, but the low concentration of this radionuclide in most of the samples precludes precise detection. Thirdly, variations in matrix composition forced by pedogenesis or cryoturbation, such as radionuclide and/or mineral remobilisation, may alter the rate of energy emission and/or absorption. However, no turbation was apparent within this study's samples. Fourthly, spatiotemporal detractions from present moisture content are difficult to assess directly, requiring knowledge of the magnitude and timing of differing contents. There is also the possibility in the present study that prior to measurement, moisture content may have reduced during storage; to counter this a 50% uncertainty has been attached to measured moisture content. The maximum influence of moisture content variations can be delimited by recalculating Dr for minimum (zero) and maximum (saturation; 40±5% for sand matrices) content. Finally, temporal alteration in the thickness of overburden alters cosmic Dr values. Cosmic Dr often forms a negligible portion of total Dr, but in the present case constitutes up to 31%. It is possible to quantify the maximum influence of overburden flux by recalculating Dr for minimum (zero) and maximum (surface sample) cosmic Dr.

6.0 Estimation of Age

Age estimates reported in Table 1 provide an estimate of sediment burial period based on mean D_e and D_r values and their associated analytical uncertainties. Uncertainty in age estimates is reported as a product of systematic and experimental errors, with the magnitude of experimental errors alone shown in parenthesis (Table 1). Probability distributions indicate the inter-aliquot variability in age (Fig. 8). The maximum influence of temporal variations in D_r forced by minima-maxima in moisture content and overburden thickness is illustrated in Fig. 8. Where uncertainty in these parameters exists this age range may prove instructive, however the combined extremes represented should not be construed as preferred age estimates. The analytical validity of each sample is presented in Table 2.

7.0 Analytical uncertainty

All errors are based upon analytical uncertainty and quoted at 1σ confidence. Error calculations account for the propagation of systematic and/or experimental (random) errors associated with D_e and D_r values.

For D_e values, systematic errors are confined to laboratory β source calibration. Uncertainty in this respect is that combined from the delivery of the calibrating γ dose (1.2%; NPL, pers. comm.), the conversion of this dose for SiO_2 using the respective mass energy-absorption coefficient (2%; Hubbell, 1982) and experimental error, totalling 3.5%. Mass attenuation and bremsstrahlung losses during γ dose delivery are considered negligible. Experimental errors relate to D_e interpolation using sensitisation corrected dose responses. Natural and regenerated sensitisation-corrected dose points (S_i) were quantified by,

$$S_i = (D_i - x.L_i) / (d_i - x.L_i)$$

Eq.1

where D_i = Natural or regenerated OSL, initial 0.2 s

L_i = Background natural or regenerated OSL, final 5 s

d_i = Test dose OSL, initial 0.2 s

x = Scaling factor, 0.08

The error on each signal parameter is based on counting statistics, reflected by the square-root of measured values. The propagation of these errors within Eq. 1 generating σS_i follows the general formula given in Eq. 2. σS_i were then used to define fitting and interpolation errors within exponential plus linear regressions.

For D_r values, systematic errors accommodate uncertainty in radionuclide conversion factors (5%), β attenuation coefficients (5%), a-value (4%; derived from a systematic α source uncertainty of 3.5% and experimental error), matrix density (0.20 $g.cm^{-3}$), vertical thickness of sampled section (specific to sample collection device), saturation moisture content (3%), moisture content attenuation (2%), burial moisture content (25% relative, unless direct evidence exists of the magnitude and period of differing content) and NaI gamma spectrometer calibration (3%). Experimental errors are associated with radionuclide quantification for each sample by NaI and Ge gamma spectrometry.

The propagation of these errors through to age calculation was quantified using the expression,

$$\sigma y\,(\delta y/\delta x) = (\Sigma\,((\delta y/\delta x_n).\sigma x_n)^2)^{1/2} \qquad \textbf{Eq. 2}$$

where y is a value equivalent to that function comprising terms x_n and where σy and σx_n are associated uncertainties.

Errors on age estimates are presented as combined systematic and experimental errors and experimental errors alone (Table 1). The former (combined) error should be considered when comparing luminescence ages herein with independent chronometric controls. The latter assumes systematic errors are common to luminescence age estimates generated by means identical to those detailed herein and enable direct comparison with those estimates.

8.0 Summary and recommendations

The Optical age estimates generated in this study, incorporating analytical uncertainties, span from 31 ka (Marine Isotope Stage 2) to greater than 869 ka (Marine Isotope Stage 24). Though all but one sample, GL10037, are accompanied by a varying range of analytical caveats, within individual cores all age estimates are consistent with their relative stratigraphic position. The antiquity of the oldest age estimates owes itself to some exceptionally low lithogenic Dr values. Whilst below average radionuclide concentrations are conducive to extending the upper age range of optical dating it should be borne in mind that age estimates become increasingly sensitive to inaccuracies in Dr as the magnitude of Dr decreases and burial period increases. The reliability of the optical chronology should be measured against any extrinsic temporal control that may be available to the project. If units dated in this study can be shown to be stratigraphically equivalent between cores then it may be possible to assess reliability intrinsically, quantifying the convergence of age estimates from divergent Dr values (Toms et al., 2005).

Field Code	Lab Code	Location	Overburden (m)	Grain size (μm)	Moisture content (%)	Ge γ-spectrometry (external γ field)			γ D_r ($Gy.ka^{-1}$)	1. GE γ-SPECTROMETRY (EXTERNAL β FIELD)			β D_r ($Gy.ka^{-1}$)	Cosmic D_r ($Gy.ka^{-1}$)	Total D_r ($Gy.ka^{-1}$)	Preheat (°C for 10s)	D_e (Gy)	Age (ka)
						K (%)	Th (ppm)	U (ppm)		K (%)	Th (ppm)	U (ppm)						
VC2b 0.85-0.95 m	GL10038	53°N, 2°E, -28m	0.90	125-180	16 ± 8	-	-	-	0.24 ± 0.05	0.65 ± 0.04	2.04 ± 0.27	0.36 ± 0.05	0.46 ± 0.07	0.18 ± 0.02	0.95 ± 0.11	260	230.1 ± 16.7	243 ± 33 (30)
VC2b 3.10-3.20 m	GL10039	53°N, 2°E, -28m	3.15	125-180	13 ± 7	0.48 ± 0.03	1.84 ± 0.27	0.40 ± 0.06	0.21 ± 0.03	0.51 ± 0.03	1.55 ± 0.27	0.33 ± 0.05	0.38 ± 0.05	0.12 ± 0.01	0.78 ± 0.07	260	326.1 ± 53.4	418 ± 78 (72)
VC3b 5.77-5.87 m	GL10040	53°N, 2°E, -28m	5.82	180-250	15 ± 8	-	-	-	0.18 ± 0.03	0.42 ± 0.03	1.59 ± 0.22	0.32 ± 0.05	0.31 ± 0.05	0.08 ± 0.01	0.63 ± 0.08	280	464.4 ± 64.0	735 ± 134 (125)
VC7b 0.45-0.55 m	GL10041	53°N, 2°E, -27m	0.50	125-180	16 ± 8	0.80 ± 0.04	3.43 ± 0.34	0.87 ± 0.07	0.37 ± 0.05	0.90 ± 0.05	3.54 ± 0.32	0.81 ± 0.07	0.68 ± 0.11	0.19 ± 0.03	1.31 ± 0.12	260	125.3 ± 8.5	96 ± 11 (9)
VC7b 1.32-1.42 m	GL10037	53°N, 2°E, -27m	1.37	125-180	13 ± 7	0.53 ± 0.03	3.63 ± 0.36	0.16 ± 0.05	0.27 ± 0.03	0.61 ± 0.04	1.81 ± 0.28	0.48 ± 0.06	0.47 ± 0.06	0.16 ± 0.02	0.96 ± 0.08	260	105.6 ± 6.2	109 ± 11 (9)
VC7b 2.50-2.65 m	GL10042	53°N, 2°E, -27m	2.57	180-250	8 ± 4	0.13 ± 0.02	0.87 ± 0.07	0.46 ± 0.05	0.12 ± 0.01	0.11 ± 0.02	0.65 ± 0.14	0.44 ± 0.05	0.13 ± 0.02	0.14 ± 0.01	0.45 ± 0.04	240	92.5 ± 6.8	207 ± 24 (18)
VC9b 0.70-0.80 m	GL10045	53°N, 2°E, -27m	0.75	180-250	12 ± 6	0.19 ± 0.02	1.49 ± 0.19	0.30 ± 0.05	0.13 ± 0.02	0.24 ± 0.02	0.89 ± 0.24	0.46 ± 0.05	0.21 ± 0.03	0.18 ± 0.03	0.59 ± 0.05	230	21.2 ± 2.3	36 ± 5 (4)
VC9b 1.45-1.55 m	GL10044	53°N, 2°E, -27m	1.50	125-180	12 ± 6	0.49 ± 0.03	1.67 ± 0.19	0.28 ± 0.05	0.20 ± 0.02	0.59 ± 0.04	1.33 ± 0.15	0.41 ± 0.05	0.44 ± 0.06	0.16 ± 0.02	0.86 ± 0.07	240	31.3 ± 1.5	36 ± 3 (3)
VC9b 4.51-4.61 m	GL10043	53°N, 2°E, -27m	4.56	125-180	15 ± 8	-	-	-	0.32 ± 0.06	0.87 ± 0.01	2.27 ± 0.33	0.58 ± 0.06	0.63 ± 0.10	0.10 ± 0.01	1.11 ± 0.14	220	313.1 ± 47.6	283 ± 56 (53)

Table 1 D_r, D_e and Age data of submitted samples. Uncertainties in age are quoted at 1σ confidence, are based on analytical errors and reflect combined systematic and experimental variability and (in parenthesis) experimental variability alone (see 6.0). Total D_r includes a standard internal α D_r of 0.06 ± 0.03 $Gy.ka^{-1}$. Blue indicates samples with accepted age estimates, red, age estimates with caveats (see Table 2).

Generic considerations	Field Code	Lab Code	Sample specific considerations
None	VC2b 0.85-0.95 m	GL10038	Overdispersion of regenerative-dose data (see 4.1.4 and Fig. 4) Significant U disequilibrium (see 5.0 and Fig. 7) Absence of γ field sample (see 5.0) Accept with strong reservations
	VC2b 3.10-3.20 m	GL10039	Overdispersion of regenerative-dose data (see 4.1.4 and Fig. 4) Accept tentatively
	VC3b 5.77-5.87 m	GL10040	Overdispersion of regenerative-dose data (see 4.1.4 and Fig. 4) Portion (25%) of aliquots saturated (see 4.1.3) Absence of γ field sample (see 5.0) Accept as minimum age estimate
	VC7b 0.45-0.55 m	GL10041	Dose Recovery test failure (see 4.1.2 and Fig. 2) Overdispersion of regenerative-dose data (see 4.1.4 and Fig. 4) Moderate U disequilibrium (see 5.0 and Fig. 7) Accept with strong reservations
	VC7b 1.32-1.42 m	GL10037	Accept
	VC7b 2.50-2.65 m	GL10042	Overdispersion of regenerative-dose data (see 4.1.4 and Fig. 4) Possible feldspar contamination (see 4.1.1 and Fig. 5) Partially bleached (see 4.2.1 and Fig. 6) Accept tentatively
	VC9b 0.70-0.80 m	GL10045	Overdispersion of regenerative-dose data (see 4.1.4 and Fig. 4) Accept tentatively
	VC9b 1.45-1.55 m	GL10044	Overdispersion of regenerative-dose data (see 4.1.4 and Fig. 4) Accept tentatively

	VC9b 4.51-4.61 m	GL10043	**Dose Recovery test failure (see 4.1.2 and Fig. 2)** **Overdispersion of regenerative-dose data (see 4.1.4 and Fig. 4)** **Possible feldspar contamination (see 4.1.1 and Fig. 5)** **Absence of γ field sample (see 5.0)** **Moderate to significant U disequilibrium (see 5.0 and Fig. 7)** **Accept with strong reservations**

Table 2 Analytical validity of sample suite age estimates and caveats for consideration

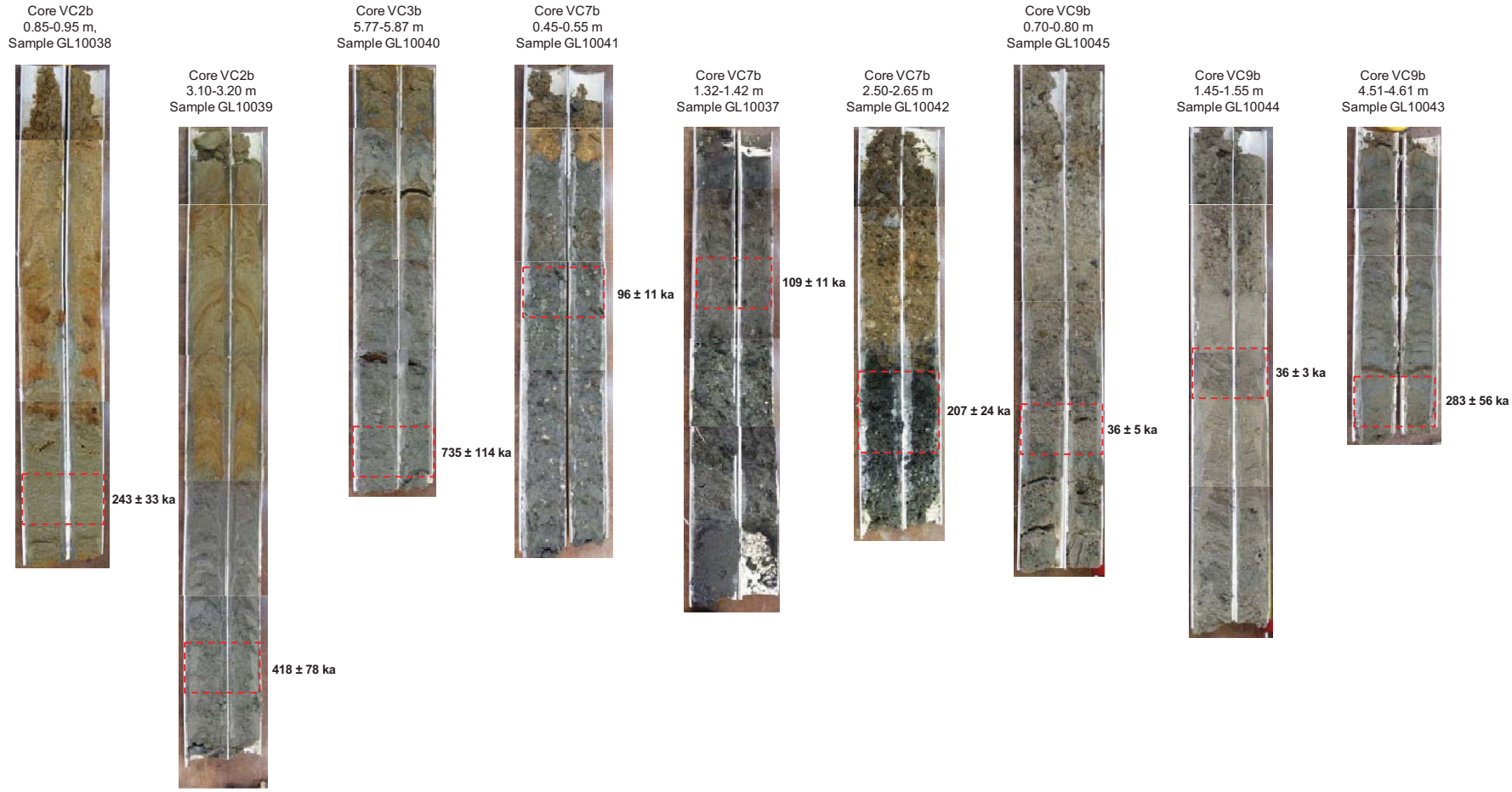

Image 1 Cores, sample positions and associated optical age estimates

Fig. 1 Signal Calibration

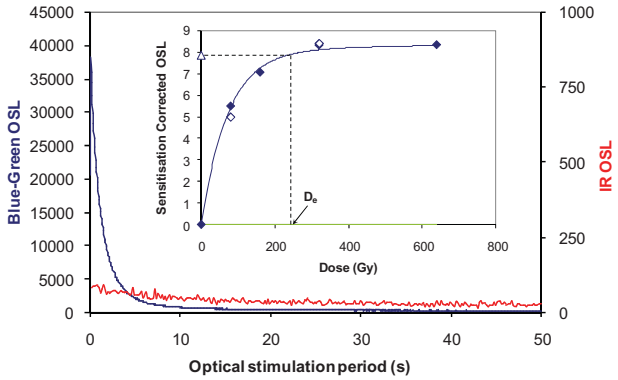

Fig. 1 Signal Calibration Natural blue and laboratory-induced infrared (IR) OSL signals. Detectable IR signal decays are diagnostic of feldspar contamination. Inset, the natural blue OSL signal (open triangle) of each aliquot is calibrated against known laboratory doses to yield equivalent dose (D_e) values. Repeats of low and high doses (open diamonds) illustrate the success of sensitivity correction.

Fig. 2 Dose Recovery The acquisition of D_e values is necessarily predicated upon thermal treatment of aliquots succeeding environmental and laboratory irradiation. The Dose Recovery test quantifies the combined effects of thermal transfer and sensitisation on the natural signal using a precise lab dose to simulate natural dose. Based on this an appropriate thermal treatment is selected to generate the final D_e value.

Fig. 3 Inter-aliquot D_e distribution Provides a measure of inter-aliquot statistical concordance in D_e values derived from **natural** irradiation. Discordant data (those points lying beyond ±2 standardised ln D_e) reflects heterogeneous dose absorption and/or inaccuracies in calibration.

Fig. 4 Low and High Repeat Regenerative-dose Ratio Measures the statistical concordance of signals from repeated **low** and **high** regenerative-doses. Discordant data (those points lying beyond ±2 standardised ln D_e) indicate inaccurate sensitivity correction.

Fig. 5 OSL to Post-IR OSL Ratio Measures the statistical concordance of OSL and post-IR OSL responses to the same regenerative-dose. Discordant, underestimating data (those points lying below -2 standardised ln D_e) highlight the presence of significant feldspar contamination.

Fig. 6 Signal Analysis Statistically significant increase in **natural** D_e value with signal stimulation period is indicative of a partially-bleached signal, provided a significant increase in D_e results from **simulated partial bleaching** followed by insignificant adjustment in D_e for simulated **zero** and **full bleach** conditions. Ages from such samples are considered maximum estimates. In the absence of a significant rise in D_e with stimulation time, simulated partial bleaching and zero/full bleach tests are not assessed.

Fig. 7 U Activity Statistical concordance (**equilibrium**) in the activities of the daughter radioisotope ^{226}Ra with its parent ^{238}U may signify the temporal stability of D_r emissions from these chains. Significant differences (disequilibrium; **>50%**) in activity indicate addition or removal of isotopes creating a time-dependent shift in D_r values and increased uncertainty in the accuracy of age estimates. A **20%** disequilibrium marker is also shown.

Fig. 8 Age Range The **mean age range** provides an estimate of sediment burial period based on mean D_e and D_r values with associated analytical uncertainties. The **probability distribution** indicates the inter-aliquot variability in age. The **maximum influence** of temporal variations in D_r forced by minima-maxima variation in moisture content and overburden thickness may prove instructive where there is uncertainty in these parameters, however the combined extremes represented should not be construed as preferred age estimates.

Fig. 2 Dose Recovery

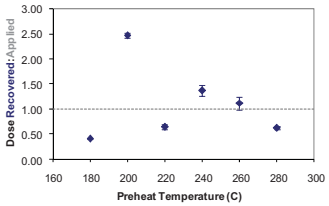

Fig. 3 Inter-aliquot D_e distribution

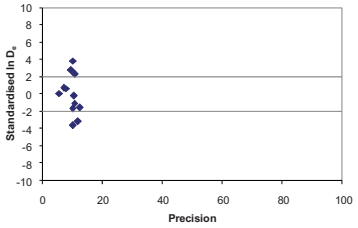

Fig. 4 Low and High Repeat Regenerative-dose Ratio

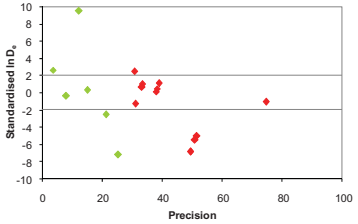

Fig. 5 OSL to Post-IR OSL Ratio

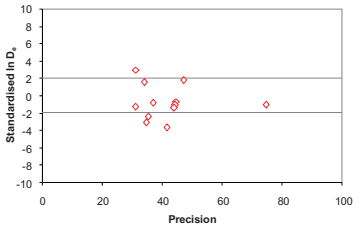

Sample: GL10038

Fig. 6 Signal Analysis

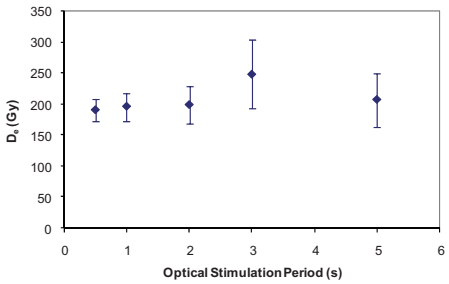

Fig. 7 U Decay Activity

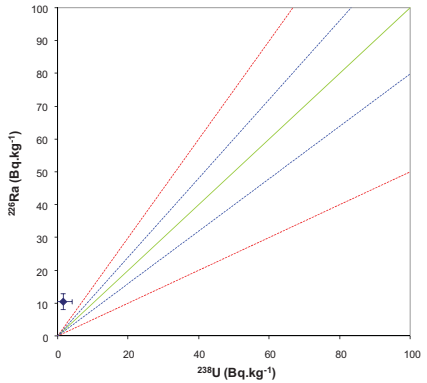

Fig. 8 Age Range

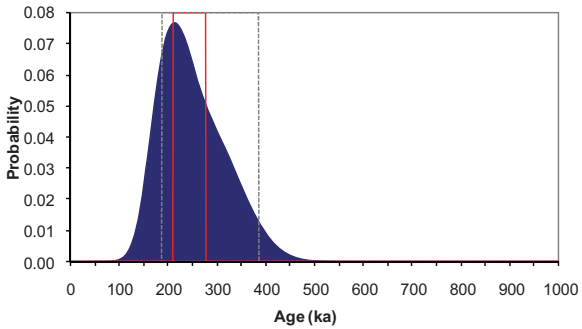

Fig. 1 Signal Calibration

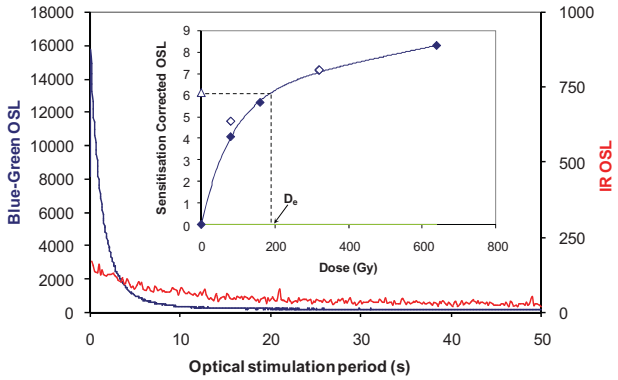

Fig. 1 Signal Calibration Natural blue and laboratory-induced infrared (IR) OSL signals. Detectable IR signal decays are diagnostic of feldspar contamination. Inset, the natural blue OSL signal (open triangle) of each aliquot is calibrated against known laboratory doses to yield equivalent dose (D_e) values. Repeats of low and high doses (open diamonds) illustrate the success of sensitivity correction.

Fig. 2 Dose Recovery The acquisition of D_e values is necessarily predicated upon thermal treatment of aliquots succeeding environmental and laboratory irradiation. The Dose Recovery test quantifies the combined effects of thermal transfer and sensitisation on the natural signal using a precise lab dose to simulate natural dose. Based on this an appropriate thermal treatment is selected to generate the final D_e value.

Fig. 3 Inter-aliquot D_e distribution Provides a measure of inter-aliquot statistical concordance in D_e values derived from **natural** irradiation. Discordant data (those points lying beyond **±2 standardised ln D_e**) reflects heterogeneous dose absorption and/or inaccuracies in calibration.

Fig. 4 Low and High Repeat Regenerative-dose Ratio Measures the statistical concordance of signals from repeated **low** and **high** regenerative-doses. Discordant data (those points lying beyond **±2 standardised ln D_e**) indicate inaccurate sensitivity correction.

Fig. 5 OSL to Post-IR OSL Ratio Measures the statistical concordance of OSL and post-IR OSL responses to the same regenerative-dose. Discordant, underestimating data (those points lying below **-2 standardised ln D_e**) highlight the presence of significant feldspar contamination.

Fig. 6 Signal Analysis Statistically significant increase in **natural** D_e value with signal stimulation period is indicative of a partially-bleached signal, provided a significant increase in D_e results from **simulated partial bleaching** followed by insignificant adjustment in D_e for simulated **zero** and **full bleach** conditions. Ages from such samples are considered maximum estimates. In the absence of a significant rise in D_e with stimulation time, simulated partial bleaching and zero/full bleach tests are not assessed.

Fig. 7 U Activity Statistical concordance (**equilibrium**) in the activities of the daughter radioisotope ^{226}Ra with its parent ^{238}U may signify the temporal stability of D_r emissions from these chains. Significant differences (disequilibrium; **>50%**) in activity indicate addition or removal of isotopes creating a time-dependent shift in D_r values and increased uncertainty in the accuracy of age estimates. A **20%** disequilibrium marker is also shown.

Fig. 8 Age Range The **mean age range** provides an estimate of sediment burial period based on mean D_e and D_r values with associated analytical uncertainties. The **probability distribution** indicates the inter-aliquot variability in age. The **maximum influence** of temporal variations in D_r forced by minima-maxima variation in moisture content and overburden thickness may prove instructive where there is uncertainty in these parameters, however the combined extremes represented should not be construed as preferred age estimates.

Fig. 2 Dose Recovery

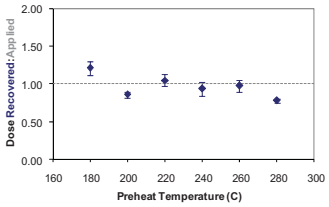

Fig. 3 Inter-aliquot D_e distribution

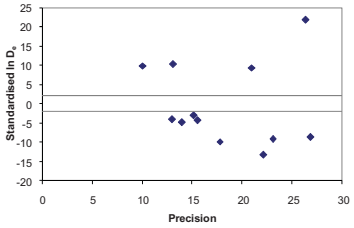

Fig. 4 Low and High Repeat Regenerative-dose Ratio

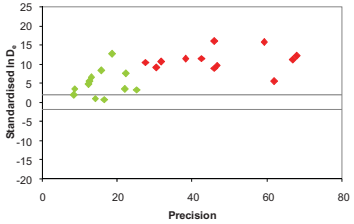

Fig. 5 OSL to Post-IR OSL Ratio

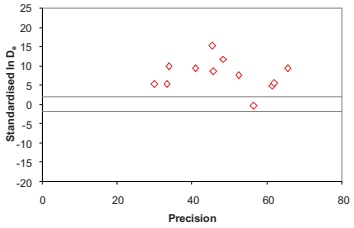

Sample: GL10039

Fig. 6 Signal Analysis

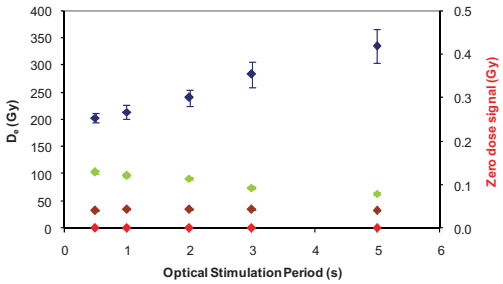

Fig. 7 U Decay Activity

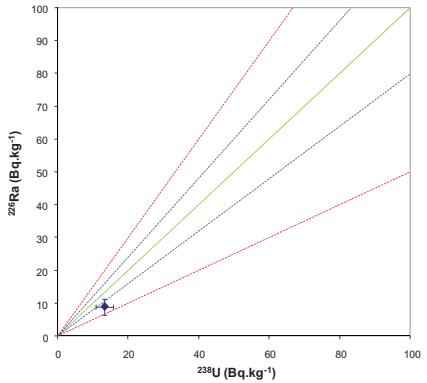

Fig. 8 Age Range

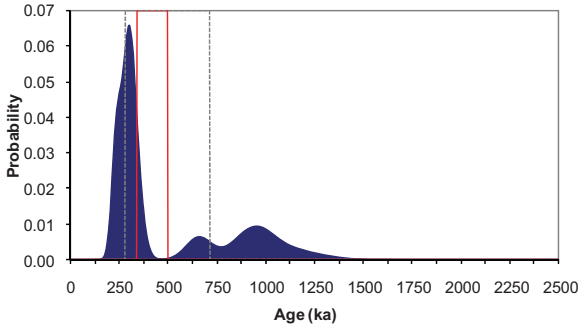

Fig. 1 Signal Calibration

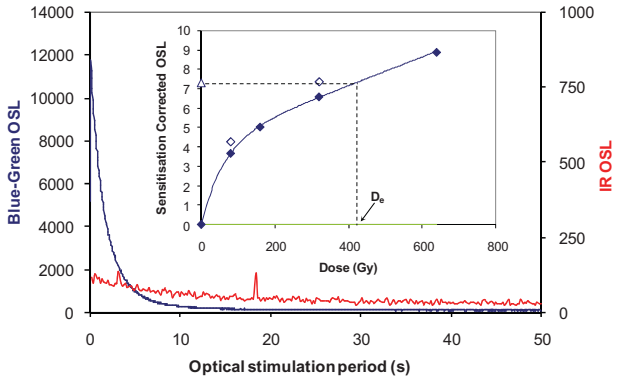

Fig. 1 Signal Calibration Natural blue and laboratory-induced infrared (IR) OSL signals. Detectable IR signal decays are diagnostic of feldspar contamination. Inset, the natural blue OSL signal (open triangle) of each aliquot is calibrated against known laboratory doses to yield equivalent dose (D_e) values. Repeats of low and high doses (open diamonds) illustrate the success of sensitivity correction.

Fig. 2 Dose Recovery The acquisition of D_e values is necessarily predicated upon thermal treatment of aliquots succeeding environmental and laboratory irradiation. The Dose Recovery test quantifies the combined effects of thermal transfer and sensitisation on the natural signal using a precise lab dose to simulate natural dose. Based on this an appropriate thermal treatment is selected to generate the final D_e value.

Fig. 3 Inter-aliquot D_e distribution Provides a measure of inter-aliquot statistical concordance in D_e values derived from **natural** irradiation. Discordant data (those points lying beyond **±2 standardised ln D_e**) reflects heterogeneous dose absorption and/or inaccuracies in calibration.

Fig. 4 Low and High Repeat Regenerative-dose Ratio Measures the statistical concordance of signals from repeated **low** and **high** regenerative-doses. Discordant data (those points lying beyond **±2 standardised ln D_e**) indicate inaccurate sensitivity correction.

Fig. 5 OSL to Post-IR OSL Ratio Measures the statistical concordance of OSL and post-IR OSL responses to the same regenerative-dose. Discordant, underestimating data (those points lying below **-2 standardised ln D_e**) highlight the presence of significant feldspar contamination.

Fig. 6 Signal Analysis Statistically significant increase in **natural** D_e value with signal stimulation period is indicative of a partially-bleached signal, provided a significant increase in D_e results from **simulated partial bleaching** followed by insignificant adjustment in D_e for simulated **zero** and **full bleach** conditions. Ages from such samples are considered maximum estimates. In the absence of a significant rise in D_e with stimulation time, simulated partial bleaching and zero/full bleach tests are not assessed.

Fig. 7 U Activity Statistical concordance (**equilibrium**) in the activities of the daughter radioisotope ^{226}Ra with its parent ^{238}U may signify the temporal stability of D_r emissions from these chains. Significant differences (disequilibrium; **>50%**) in activity indicate addition or removal of isotopes creating a time-dependent shift in D_r values and increased uncertainty in the accuracy of age estimates. A **20%** disequilibrium marker is also shown.

Fig. 8 Age Range The **mean age range** provides an estimate of sediment burial period based on mean D_e and D_r values with associated analytical uncertainties. The **probability distribution** indicates the inter-aliquot variability in age. The **maximum influence** of temporal variations in D_r forced by minima-maxima variation in moisture content and overburden thickness may prove instructive where there is uncertainty in these parameters, however the combined extremes represented should not be construed as preferred age estimates.

Fig. 2 Dose Recovery

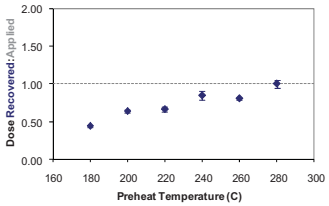

Fig. 3 Inter-aliquot D_e distribution

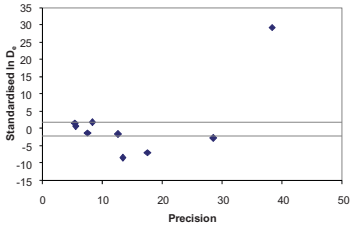

Fig. 4 Low and High Repeat Regenerative-dose Ratio

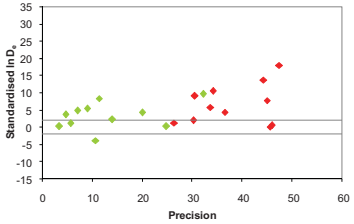

Fig. 5 OSL to Post-IR OSL Ratio

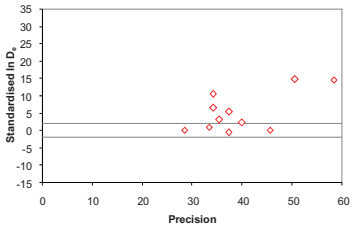

Sample: GL10040

Fig. 6 Signal Analysis

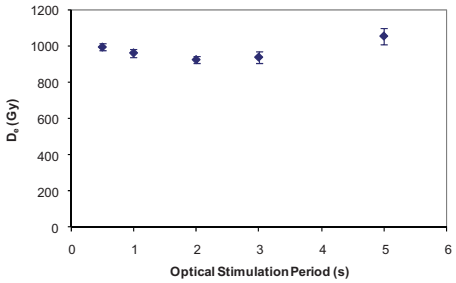

Fig. 7 U Decay Activity

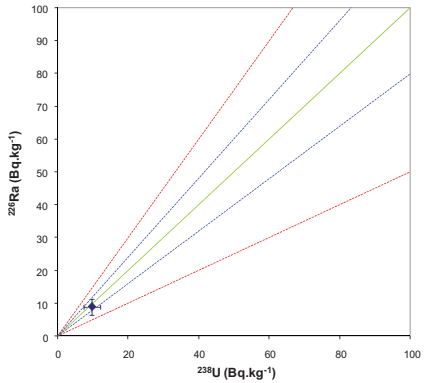

Fig. 8 Age Range

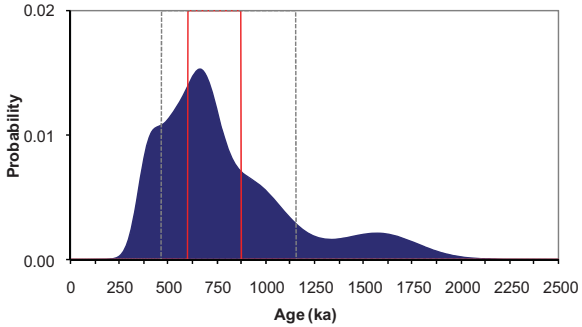

Fig. 1 Signal Calibration

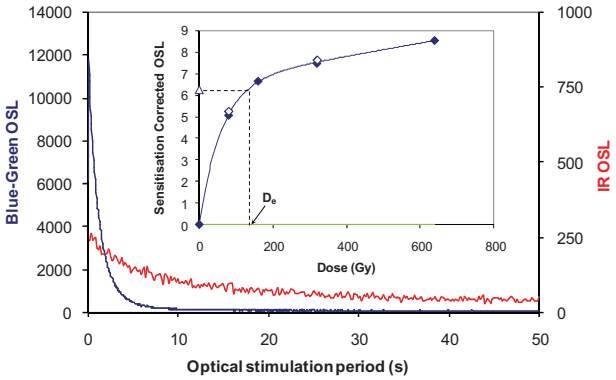

Fig. 1 Signal Calibration Natural blue and laboratory-induced infrared (IR) OSL signals. Detectable IR signal decays are diagnostic of feldspar contamination. Inset, the natural blue OSL signal (open triangle) of each aliquot is calibrated against known laboratory doses to yield equivalent dose (D_e) values. Repeats of low and high doses (open diamonds) illustrate the success of sensitivity correction.

Fig. 2 Dose Recovery The acquisition of D_e values is necessarily predicated upon thermal treatment of aliquots succeeding environmental and laboratory irradiation. The Dose Recovery test quantifies the combined effects of thermal transfer and sensitisation on the natural signal using a precise lab dose to simulate natural dose. Based on this an appropriate thermal treatment is selected to generate the final D_e value.

Fig. 3 Inter-aliquot D_e distribution Provides a measure of inter-aliquot statistical concordance in D_e values derived from **natural** irradiation. Discordant data (those points lying beyond **±2 standardised ln D_e**) reflects heterogeneous dose absorption and/or inaccuracies in calibration.

Fig. 4 Low and High Repeat Regenerative-dose Ratio Measures the statistical concordance of signals from repeated **low** and **high** regenerative-doses. Discordant data (those points lying beyond **±2 standardised ln D_e**) indicate inaccurate sensitivity correction.

Fig. 5 OSL to Post-IR OSL Ratio Measures the statistical concordance of OSL and post-IR OSL responses to the same regenerative-dose. Discordant, underestimating data (those points lying below **-2 standardised ln D_e**) highlight the presence of significant feldspar contamination.

Fig. 6 Signal Analysis Statistically significant increase in **natural** D_e value with signal stimulation period is indicative of a partially-bleached signal, provided a significant increase in D_e results from **simulated partial bleaching** followed by insignificant adjustment in D_e for simulated **zero** and **full bleach** conditions. Ages from such samples are considered maximum estimates. In the absence of a significant rise in D_e with stimulation time, simulated partial bleaching and zero/full bleach tests are not assessed.

Fig. 7 U Activity Statistical concordance (**equilibrium**) in the activities of the daughter radioisotope ^{226}Ra with its parent ^{238}U may signify the temporal stability of D_r emissions from these chains. Significant differences (disequilibrium; **>50%**) in activity indicate addition or removal of isotopes creating a time-dependent shift in D_r values and increased uncertainty in the accuracy of age estimates. A **20%** disequilibrium marker is also shown.

Fig. 8 Age Range The **mean age range** provides an estimate of sediment burial period based on mean D_e and D_r values with associated analytical uncertainties. The **probability distribution** indicates the inter-aliquot variability in age. The **maximum influence** of temporal variations in D_r forced by minima-maxima variation in moisture content and overburden thickness may prove instructive where there is uncertainty in these parameters, however the combined extremes represented should not be construed as preferred age estimates.

Fig. 2 Dose Recovery

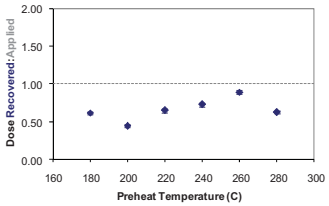

Fig. 3 Inter-aliquot D_e distribution

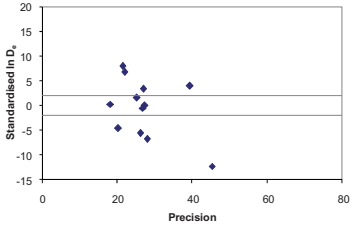

Fig. 4 Low and High Repeat Regenerative-dose Ratio

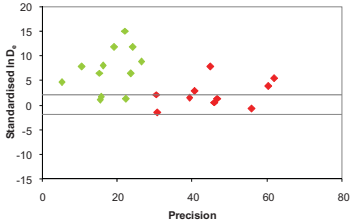

Fig. 5 OSL to Post-IR OSL Ratio

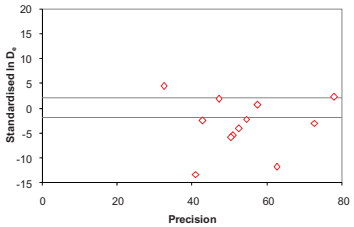

Sample: GL10041

Fig. 6 Signal Analysis

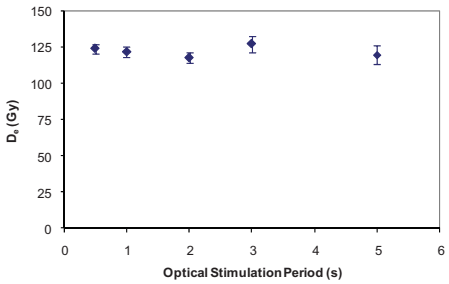

Fig. 7 U Decay Activity

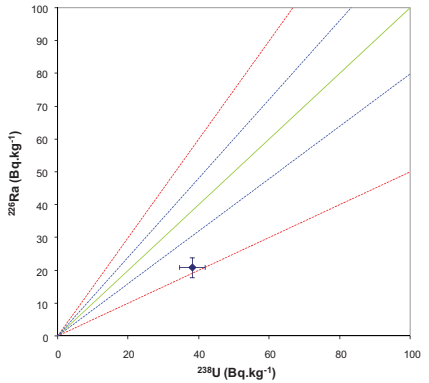

Fig. 8 Age Range

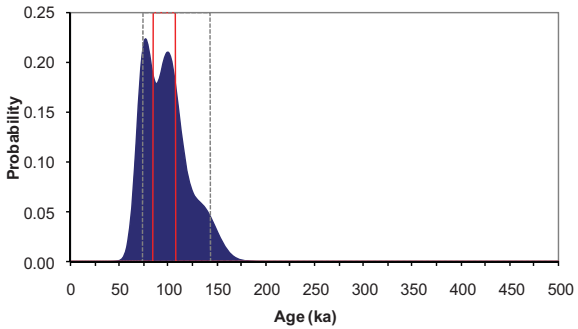

Fig. 1 Signal Calibration

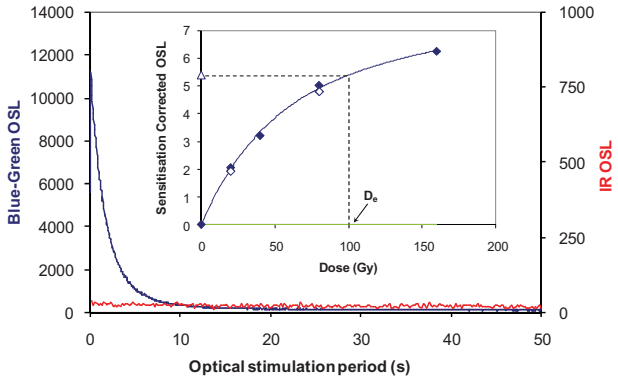

Fig. 1 Signal Calibration Natural blue and laboratory-induced infrared (IR) OSL signals. Detectable IR signal decays are diagnostic of feldspar contamination. Inset, the natural blue OSL signal (open triangle) of each aliquot is calibrated against known laboratory doses to yield equivalent dose (D_e) values. Repeats of low and high doses (open diamonds) illustrate the success of sensitivity correction.

Fig. 2 Dose Recovery The acquisition of D_e values is necessarily predicated upon thermal treatment of aliquots succeeding environmental and laboratory irradiation. The Dose Recovery test quantifies the combined effects of thermal transfer and sensitisation on the natural signal using a precise lab dose to simulate natural dose. Based on this an appropriate thermal treatment is selected to generate the final D_e value.

Fig. 3 Inter-aliquot D_e distribution Provides a measure of inter-aliquot statistical concordance in D_e values derived from **natural** irradiation. Discordant data (those points lying beyond **±2 standardised ln D_e**) reflects heterogeneous dose absorption and/or inaccuracies in calibration.

Fig. 4 Low and High Repeat Regenerative-dose Ratio Measures the statistical concordance of signals from repeated **low** and **high** regenerative-doses. Discordant data (those points lying beyond **±2 standardised ln D_e**) indicate inaccurate sensitivity correction.

Fig. 5 OSL to Post-IR OSL Ratio Measures the statistical concordance of OSL and post-IR OSL responses to the same regenerative-dose. Discordant, underestimating data (those points lying below **-2 standardised ln D_e**) highlight the presence of significant feldspar contamination.

Fig. 6 Signal Analysis Statistically significant increase in **natural** D_e value with signal stimulation period is indicative of a partially-bleached signal, provided a significant increase in D_e results from **simulated partial bleaching** followed by insignificant adjustment in D_e for simulated **zero** and **full bleach** conditions. Ages from such samples are considered maximum estimates. In the absence of a significant rise in D_e with stimulation time, simulated partial bleaching and zero/full bleach tests are not assessed.

Fig. 7 U Activity Statistical concordance (**equilibrium**) in the activities of the daughter radioisotope ^{226}Ra with its parent ^{238}U may signify the temporal stability of D_r emissions from these chains. Significant differences (disequilibrium; **>50%**) in activity indicate addition or removal of isotopes creating a time-dependent shift in D_r values and increased uncertainty in the accuracy of age estimates. A **20%** disequilibrium marker is also shown.

Fig. 8 Age Range The **mean age range** provides an estimate of sediment burial period based on mean D_e and D_r values with associated analytical uncertainties. The **probability distribution** indicates the inter-aliquot variability in age. The **maximum influence** of temporal variations in D_r forced by minima-maxima variation in moisture content and overburden thickness may prove instructive where there is uncertainty in these parameters, however the combined extremes represented should not be construed as preferred age estimates.

Fig. 2 Dose Recovery

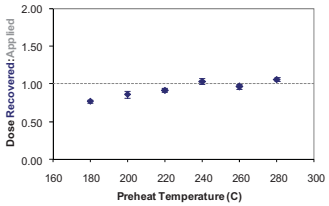

Fig. 3 Inter-aliquot D_e distribution

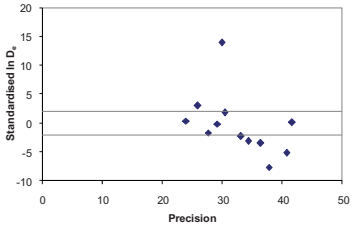

Fig. 4 Low and High Repeat Regenerative-dose Ratio

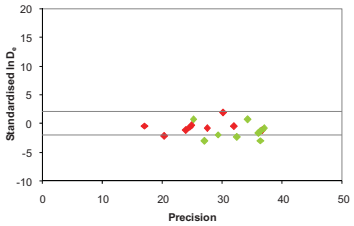

Fig. 5 OSL to Post-IR OSL Ratio

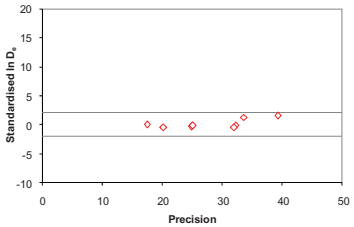

Sample: GL10037

Fig. 6 Signal Analysis

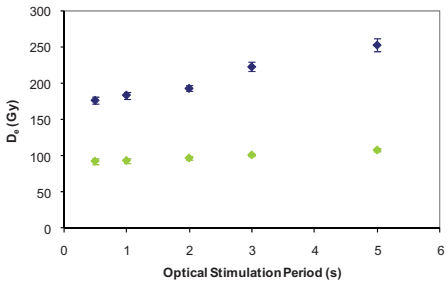

Fig. 7 U Decay Activity

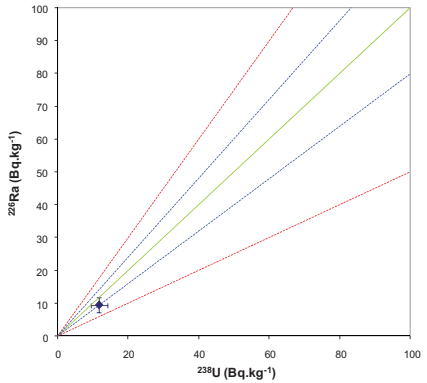

Fig. 8 Age Range

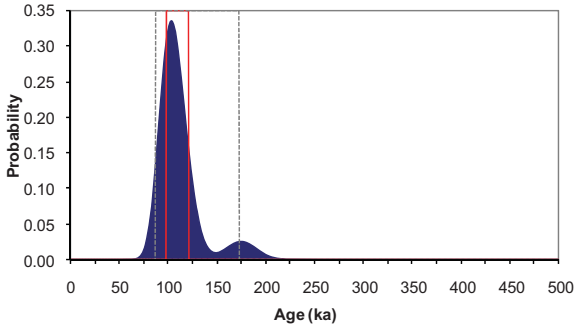

Fig. 1 Signal Calibration

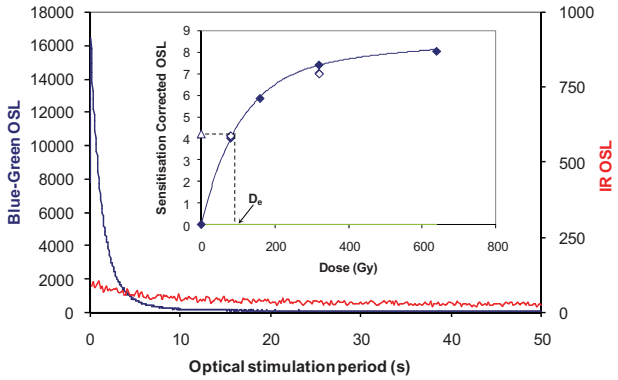

Fig. 1 Signal Calibration Natural blue and laboratory-induced infrared (IR) OSL signals. Detectable IR signal decays are diagnostic of feldspar contamination. Inset, the natural blue OSL signal (open triangle) of each aliquot is calibrated against known laboratory doses to yield equivalent dose (D_e) values. Repeats of low and high doses (open diamonds) illustrate the success of sensitivity correction.

Fig. 2 Dose Recovery The acquisition of D_e values is necessarily predicated upon thermal treatment of aliquots succeeding environmental and laboratory irradiation. The Dose Recovery test quantifies the combined effects of thermal transfer and sensitisation on the natural signal using a precise lab dose to simulate natural dose. Based on this an appropriate thermal treatment is selected to generate the final D_e value.

Fig. 3 Inter-aliquot D_e distribution Provides a measure of inter-aliquot statistical concordance in D_e values derived from **natural** irradiation. Discordant data (those points lying beyond ±2 standardised ln D_e) reflects heterogeneous dose absorption and/or inaccuracies in calibration.

Fig. 4 Low and High Repeat Regenerative-dose Ratio Measures the statistical concordance of signals from repeated **low** and **high** regenerative-doses. Discordant data (those points lying beyond ±2 standardised ln D_e) indicate inaccurate sensitivity correction.

Fig. 5 OSL to Post-IR OSL Ratio Measures the statistical concordance of OSL and post-IR OSL responses to the same regenerative-dose. Discordant, underestimating data (those points lying below -2 standardised ln D_e) highlight the presence of significant feldspar contamination.

Fig. 6 Signal Analysis Statistically significant increase in **natural** D_e value with signal stimulation period is indicative of a partially-bleached signal, provided a significant increase in D_e results from **simulated partial bleaching** followed by insignificant adjustment in D_e for simulated **zero** and **full bleach** conditions. Ages from such samples are considered maximum estimates. In the absence of a significant rise in D_e with stimulation time, simulated partial bleaching and zero/full bleach tests are not assessed.

Fig. 7 U Activity Statistical concordance (**equilibrium**) in the activities of the daughter radioisotope ^{226}Ra with its parent ^{238}U may signify the temporal stability of D_r emissions from these chains. Significant differences (disequilibrium; **>50%**) in activity indicate addition or removal of isotopes creating a time-dependent shift in D_r values and increased uncertainty in the accuracy of age estimates. A **20%** disequilibrium marker is also shown.

Fig. 8 Age Range The **mean age range** provides an estimate of sediment burial period based on mean D_e and D_r values with associated analytical uncertainties. The **probability distribution** indicates the inter-aliquot variability in age. The **maximum influence** of temporal variations in D_r forced by minima-maxima variation in moisture content and overburden thickness may prove instructive where there is uncertainty in these parameters, however the combined extremes represented should not be construed as preferred age estimates.

Fig. 2 Dose Recovery

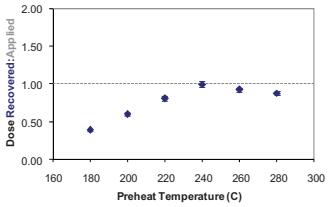

Fig. 3 Inter-aliquot D_e distribution

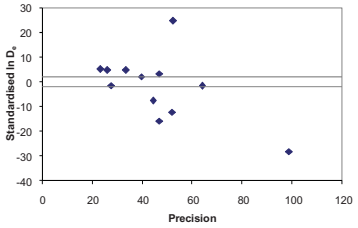

Fig. 4 Low and High Repeat Regenerative-dose Ratio

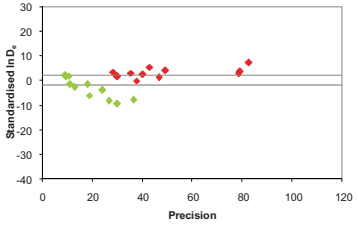

Fig. 5 OSL to Post-IR OSL Ratio

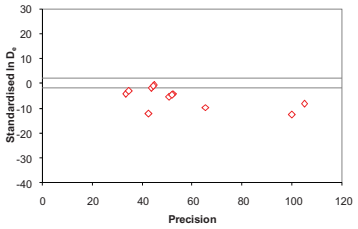

Sample: GL10042

Fig. 6 Signal Analysis

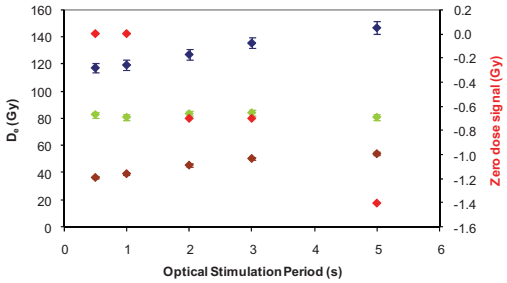

Fig. 7 U Decay Activity

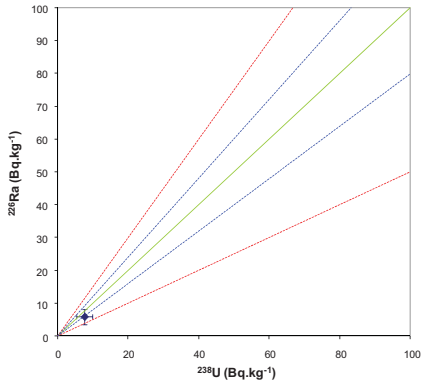

Fig. 8 Age Range

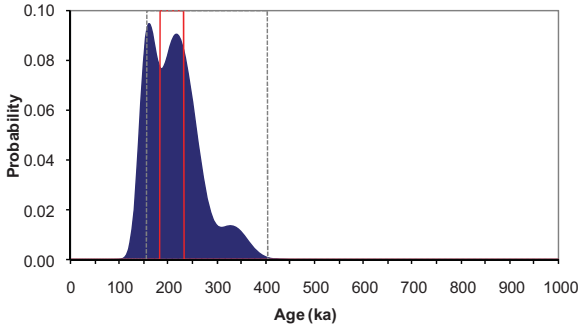

Fig. 1 Signal Calibration

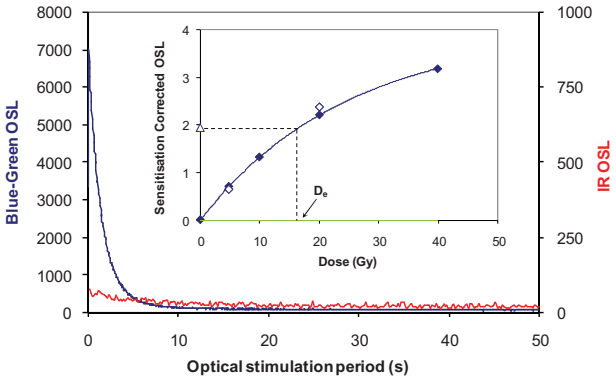

Fig. 1 Signal Calibration Natural blue and laboratory-induced infrared (IR) OSL signals. Detectable IR signal decays are diagnostic of feldspar contamination. Inset, the natural blue OSL signal (open triangle) of each aliquot is calibrated against known laboratory doses to yield equivalent dose (D_e) values. Repeats of low and high doses (open diamonds) illustrate the success of sensitivity correction.

Fig. 2 Dose Recovery The acquisition of D_e values is necessarily predicated upon thermal treatment of aliquots succeeding environmental and laboratory irradiation. The Dose Recovery test quantifies the combined effects of thermal transfer and sensitisation on the natural signal using a precise lab dose to simulate natural dose. Based on this an appropriate thermal treatment is selected to generate the final D_e value.

Fig. 3 Inter-aliquot D_e distribution Provides a measure of inter-aliquot statistical concordance in D_e values derived from **natural** irradiation. Discordant data (those points lying beyond ±2 standardised ln D_e) reflects heterogeneous dose absorption and/or inaccuracies in calibration.

Fig. 4 Low and High Repeat Regenerative-dose Ratio Measures the statistical concordance of signals from repeated **low** and **high** regenerative-doses. Discordant data (those points lying beyond ±2 standardised ln D_e) indicate inaccurate sensitivity correction.

Fig. 5 OSL to Post-IR OSL Ratio Measures the statistical concordance of OSL and post-IR OSL responses to the same regenerative-dose. Discordant, underestimating data (those points lying below -2 standardised ln D_e) highlight the presence of significant feldspar contamination.

Fig. 6 Signal Analysis Statistically significant increase in **natural** D_e value with signal stimulation period is indicative of a partially-bleached signal, provided a significant increase in D_e results from **simulated partial bleaching** followed by insignificant adjustment in D_e for simulated **zero** and **full bleach** conditions. Ages from such samples are considered maximum estimates. In the absence of a significant rise in D_e with stimulation time, simulated partial bleaching and zero/full bleach tests are not assessed.

Fig. 7 U Activity Statistical concordance (**equilibrium**) in the activities of the daughter radioisotope ^{226}Ra with its parent ^{238}U may signify the temporal stability of D_r emissions from these chains. Significant differences (disequilibrium; **>50%**) in activity indicate addition or removal of isotopes creating a time-dependent shift in D_r values and increased uncertainty in the accuracy of age estimates. A **20%** disequilibrium marker is also shown.

Fig. 8 Age Range The **mean age range** provides an estimate of sediment burial period based on mean D_e and D_r values with associated analytical uncertainties. The **probability distribution** indicates the inter-aliquot variability in age. The **maximum influence** of temporal variations in D_r forced by minima-maxima variation in moisture content and overburden thickness may prove instructive where there is uncertainty in these parameters, however the combined extremes represented should not be construed as preferred age estimates.

Fig. 2 Dose Recovery

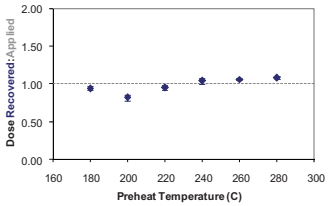

Fig. 3 Inter-aliquot D_e distribution

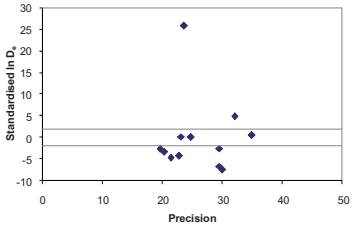

Fig. 4 Low and High Repeat Regenerative-dose Ratio

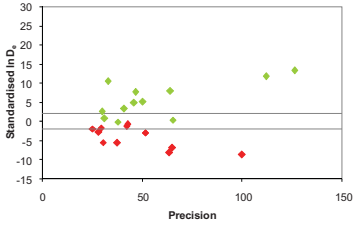

Fig. 5 OSL to Post-IR OSL Ratio

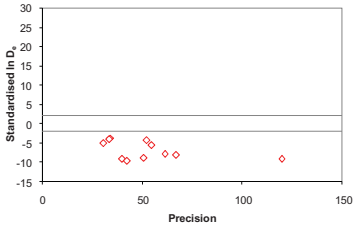

Sample: GL10045

Fig. 6 Signal Analysis

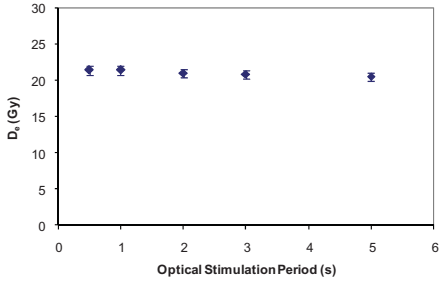

Fig. 7 U Decay Activity

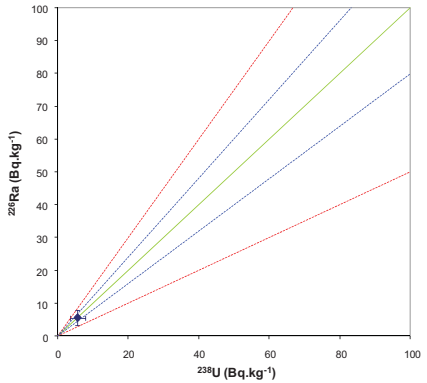

Fig. 8 Age Range

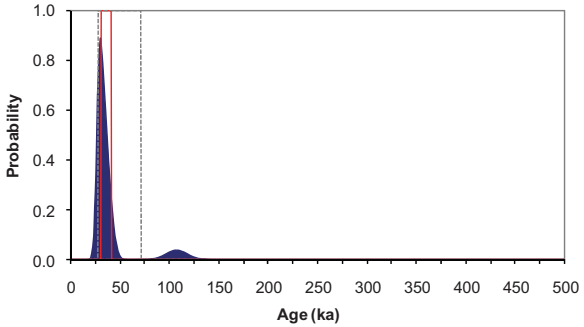

Fig. 1 Signal Calibration

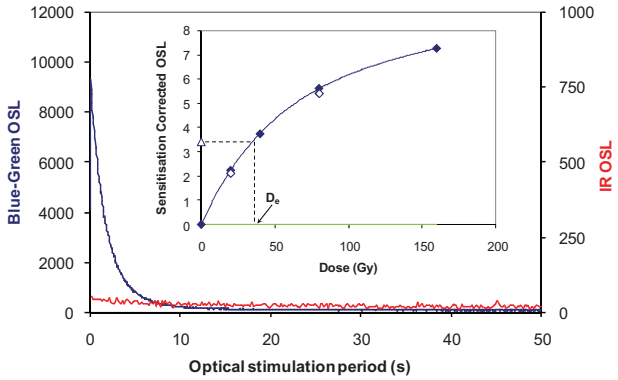

Fig. 1 Signal Calibration Natural blue and laboratory-induced infrared (IR) OSL signals. Detectable IR signal decays are diagnostic of feldspar contamination. Inset, the natural blue OSL signal (open triangle) of each aliquot is calibrated against known laboratory doses to yield equivalent dose (D_e) values. Repeats of low and high doses (open diamonds) illustrate the success of sensitivity correction.

Fig. 2 Dose Recovery The acquisition of D_e values is necessarily predicated upon thermal treatment of aliquots succeeding environmental and laboratory irradiation. The Dose Recovery test quantifies the combined effects of thermal transfer and sensitisation on the natural signal using a precise lab dose to simulate natural dose. Based on this an appropriate thermal treatment is selected to generate the final D_e value.

Fig. 3 Inter-aliquot D_e distribution Provides a measure of inter-aliquot statistical concordance in D_e values derived from **natural** irradiation. Discordant data (those points lying beyond ±2 standardised ln D_e) reflects heterogeneous dose absorption and/or inaccuracies in calibration.

Fig. 4 Low and High Repeat Regenerative-dose Ratio Measures the statistical concordance of signals from repeated **low** and **high** regenerative-doses. Discordant data (those points lying beyond ±2 standardised ln D_e) indicate inaccurate sensitivity correction.

Fig. 5 OSL to Post-IR OSL Ratio Measures the statistical concordance of OSL and post-IR OSL responses to the same regenerative-dose. Discordant, underestimating data (those points lying below -2 standardised ln D_e) highlight the presence of significant feldspar contamination.

Fig. 6 Signal Analysis Statistically significant increase in **natural** D_e value with signal stimulation period is indicative of a partially-bleached signal, provided a significant increase in D_e results from **simulated partial bleaching** followed by insignificant adjustment in D_e for simulated **zero** and **full bleach** conditions. Ages from such samples are considered maximum estimates. In the absence of a significant rise in D_e with stimulation time, simulated partial bleaching and zero/full bleach tests are not assessed.

Fig. 7 U Activity Statistical concordance (**equilibrium**) in the activities of the daughter radioisotope ^{226}Ra with its parent ^{238}U may signify the temporal stability of D_r emissions from these chains. Significant differences (disequilibrium; **>50%**) in activity indicate addition or removal of isotopes creating a time-dependent shift in D_r values and increased uncertainty in the accuracy of age estimates. A **20%** disequilibrium marker is also shown.

Fig. 8 Age Range The **mean age range** provides an estimate of sediment burial period based on mean D_e and D_r values with associated analytical uncertainties. The **probability distribution** indicates the inter-aliquot variability in age. The **maximum influence** of temporal variations in D_r forced by minima-maxima variation in moisture content and overburden thickness may prove instructive where there is uncertainty in these parameters, however the combined extremes represented should not be construed as preferred age estimates.

Fig. 2 Dose Recovery

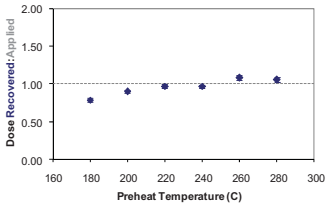

Fig. 3 Inter-aliquot D_e distribution

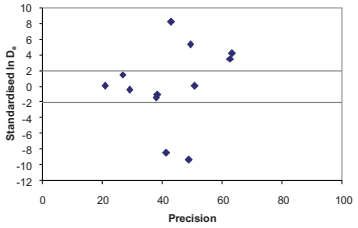

Fig. 4 Low and High Repeat Regenerative-dose Ratio

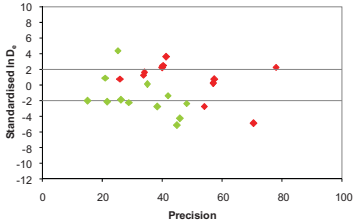

Fig. 5 OSL to Post-IR OSL Ratio

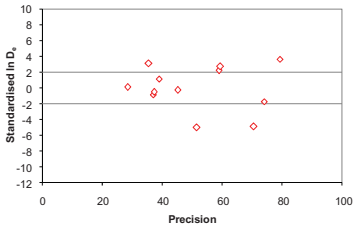

Sample: GL10044

Fig. 6 Signal Analysis

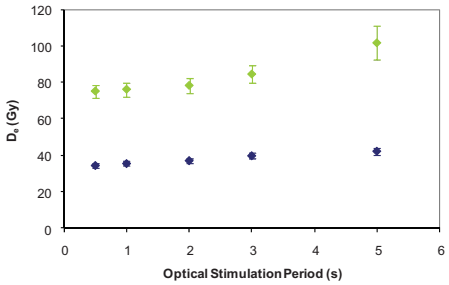

Fig. 7 U Decay Activity

^{226}Ra activity beneath detection limits

Fig. 8 Age Range

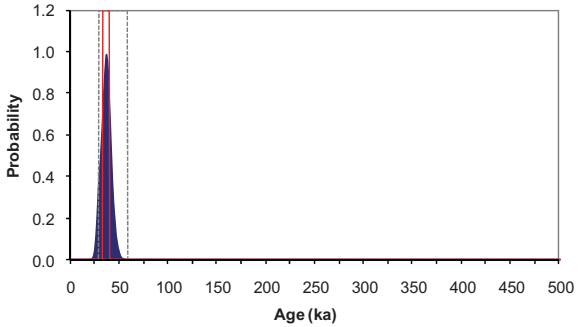

Fig. 1 Signal Calibration

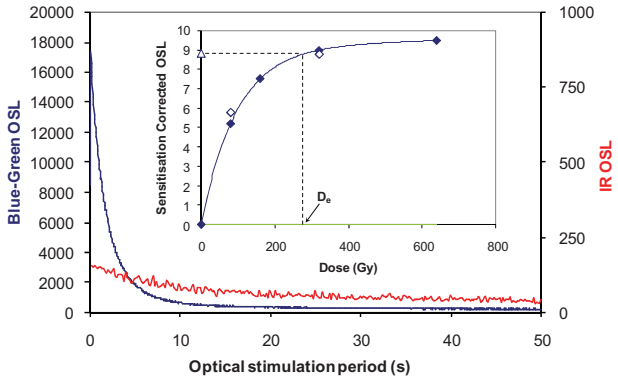

Fig. 1 Signal Calibration Natural blue and laboratory-induced infrared (IR) OSL signals. Detectable IR signal decays are diagnostic of feldspar contamination. Inset, the natural blue OSL signal (open triangle) of each aliquot is calibrated against known laboratory doses to yield equivalent dose (D_e) values. Repeats of low and high doses (open diamonds) illustrate the success of sensitivity correction.

Fig. 2 Dose Recovery The acquisition of D_e values is necessarily predicated upon thermal treatment of aliquots succeeding environmental and laboratory irradiation. The Dose Recovery test quantifies the combined effects of thermal transfer and sensitisation on the natural signal using a precise lab dose to simulate natural dose. Based on this an appropriate thermal treatment is selected to generate the final D_e value.

Fig. 3 Inter-aliquot D_e distribution Provides a measure of inter-aliquot statistical concordance in D_e values derived from **natural** irradiation. Discordant data (those points lying beyond **±2 standardised ln D_e**) reflects heterogeneous dose absorption and/or inaccuracies in calibration.

Fig. 4 Low and High Repeat Regenerative-dose Ratio Measures the statistical concordance of signals from repeated **low** and **high** regenerative-doses. Discordant data (those points lying beyond **±2 standardised ln D_e**) indicate inaccurate sensitivity correction.

Fig. 5 OSL to Post-IR OSL Ratio Measures the statistical concordance of OSL and post-IR OSL responses to the same regenerative-dose. Discordant, underestimating data (those points lying below **-2 standardised ln D_e**) highlight the presence of significant feldspar contamination.

Fig. 6 Signal Analysis Statistically significant increase in **natural** D_e value with signal stimulation period is indicative of a partially-bleached signal, provided a significant increase in D_e results from **simulated partial bleaching** followed by insignificant adjustment in D_e for simulated **zero** and **full bleach** conditions. Ages from such samples are considered maximum estimates. In the absence of a significant rise in D_e with stimulation time, simulated partial bleaching and zero/full bleach tests are not assessed.

Fig. 7 U Activity Statistical concordance (**equilibrium**) in the activities of the daughter radioisotope ^{226}Ra with its parent ^{238}U may signify the temporal stability of D_r emissions from these chains. Significant differences (disequilibrium; **>50%**) in activity indicate addition or removal of isotopes creating a time-dependent shift in D_r values and increased uncertainty in the accuracy of age estimates. A **20%** disequilibrium marker is also shown.

Fig. 8 Age Range The **mean age range** provides an estimate of sediment burial period based on mean D_e and D_r values with associated analytical uncertainties. The **probability distribution** indicates the inter-aliquot variability in age. The **maximum influence** of temporal variations in D_r forced by minima-maxima variation in moisture content and overburden thickness may prove instructive where there is uncertainty in these parameters, however the combined extremes represented should not be construed as preferred age estimates.

Fig. 2 Dose Recovery

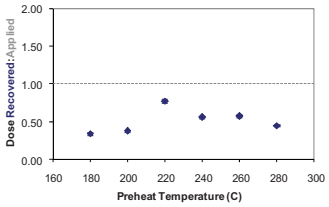

Fig. 3 Inter-aliquot D_e distribution

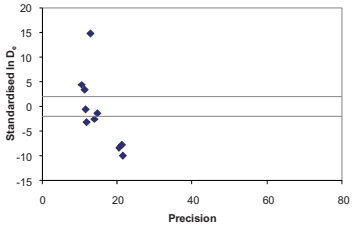

Fig. 4 Low and High Repeat Regenerative-dose Ratio

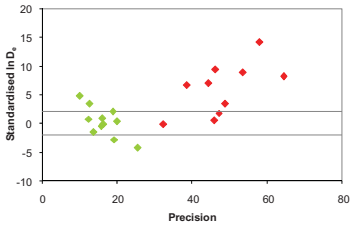

Fig. 5 OSL to Post-IR OSL Ratio

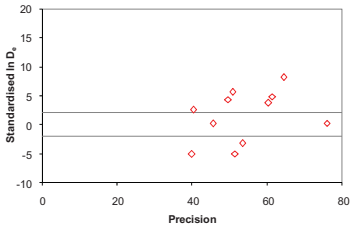

Sample: GL10043

Fig. 6 Signal Analysis

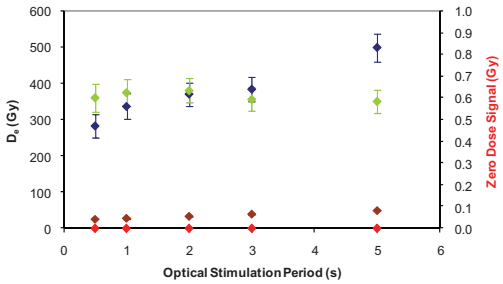

Fig. 7 U Decay Activity

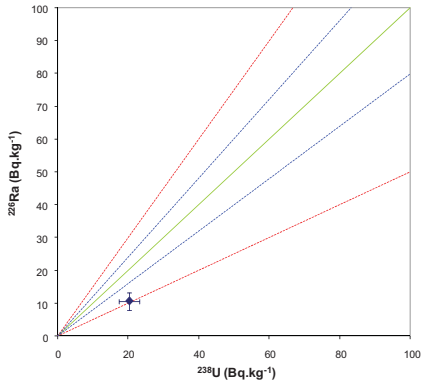

Fig. 8 Age Range

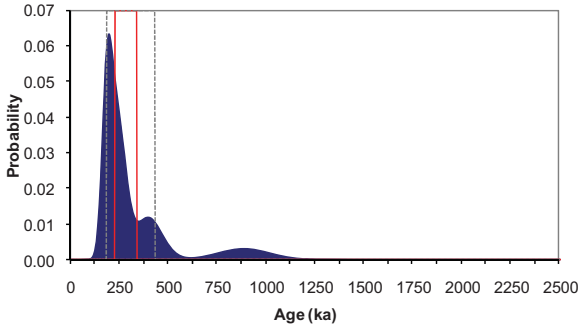

References

Adamiec, G. and Aitken, M.J., 1998. Dose-rate conversion factors: new data. *Ancient TL*, 16, 37-50.

Agersnap-Larsen, N., Bulur, E., Bøtter-Jensen, L. and McKeever, S.W.S., 2000. Use of the LM-OSL technique for the detection of partial bleaching in quartz. *Radiation Measurements*, 32, 419-425.

Aitken, M.J.,1985. Thermoluminescence dating. Academic Press.

Aitken, M. J., 1998. An introduction to optical dating: the dating of Quaternary sediments by the use of photon-stimulated luminescence. Oxford University Press.

Bailey, R.M., Singarayer, J.S. , Ward, S. and Stokes, S., 2003. Identification of partial resetting using D_e as a function of illumination time. *Radiation Measurements*, 37, 511-518.

Banerjee, D., Murray, A.S., Bøtter-Jensen, L. and Lang, A., 2001. Equivalent dose estimation using a single aliquot of polymineral fine grains. *Radiation Measurements*, 33, 73-94.

Bateman, M.D., Frederick, C.D., Jaiswal, M.K., Singhvi, A.K., 2003. Investigations into the potential effects of pedoturbation on luminescence dating. *Quaternary Science Reviews*, 22, 1169-1176.

Bøtter-Jensen, L., Mejdahl, V. and Murray, A.S., 1999. New light on OSL. *Quaternary Science Reviews*, 18, 303-310.

Bøtter-Jensen, L., McKeever, S.W.S. and Wintle, A.G., 2003. Optically Stimulated Luminescence Dosimetry. Elsevier, Amsterdam.

Duller, G.A.T, 2003. Distinguishing quartz and feldspar in single grain luminescence measurements. *Radiation Measurements*, 37, 161-165.

Galbraith, R, F., 1990. The radial plot: graphical assessment of spread in ages. *Nuclear Tracks and Radiation Measurements*, 17, 207-214.

Galbraith, R. F., Roberts, R. G., Laslett, G. M., Yoshida, H. and Olley, J. M., 1999. Optical dating of single and multiple grains of quartz from Jinmium rock shelter (northern Australia): Part I, Experimental design and statistical models. *Archaeometry*, 41, 339-364.

Hubble, J. H., 1982. Photon mass attenuation and energy-absorption coefficients from 1keV to 20MeV. *International Journal of Applied Radioisotopes*, 33, 1269-1290.

Huntley, D.J., Godfrey-Smith, D.I. and Thewalt, M.L.W., 1985. Optical dating of sediments. *Nature*, 313, 105-107.

Hütt, G., Jaek, I. and Tchonka, J., 1988. Optical dating: K-feldspars optical response stimulation spectra. *Quaternary Science Reviews*, 7, 381-386.

Jakobsen, M., Backman, J., Murray, A. and Reidar, L., 2003. Optically Stimulated Luminescence dating supports central Arctic Ocean cm-scale sedimentation rates. Geochemistry, Geophysics, Geosystems, 4, 1016.

Markey, B.G., Bøtter-Jensen, L., and Duller, G.A.T., 1997. A new flexible system for measuring thermally and optically stimulated luminescence. *Radiation Measurements*, 27, 83-89.

Mejdahl, V.,1979. Thermoluminescence dating: beta-dose attenuation in quartz grains. *Archaeometry*, 21, 61-72.

Murray, A.S. and Olley, J.M., 2002. Precision and accuracy in the Optically Stimulated Luminescence dating of sedimentary quartz: a status review. *Geochronometria*, 21, 1-16.

Murray, A.S. and Wintle, A.G., 2000. Luminescence dating of quartz using an improved single-aliquot regenerative-dose protocol. *Radiation Measurements*, 32, 57-73.

Murray, A.S. and Wintle, A.G., 2003. The single aliquot regenerative dose protocol: potential for improvements in reliability. *Radiation Measurements*, 37, 377-381.

Murray, A.S., Olley, J.M. and Caitcheon, G.G., 1995. Measurement of equivalent doses in quartz from contemporary water-lain sediments using optically stimulated luminescence. *Quaternary Science Reviews*, 14, 365-371.

Murray, A.S., Wintle, A.G., and Wallinga, J., 2002. Dose estimation using quartz OSL in the non-linear region of the growth curve. *Radiation Protection Dosimetry*, 101, 371-374.

Olley, J.M., Murray, A.S. and Roberts, R.G., 1996. The effects of disequilibria in the Uranium and Thorium decay chains on burial dose rates in fluvial sediments. *Quaternary Science Reviews*, 15, 751-760.

Olley, J.M., Caitcheon, G.G. and Murray, A.S. , 1998. The distribution of apparent dose as determined by optically stimulated luminescence in small aliquots of fluvial quartz: implications for dating young sediments. *Quaternary Science Reviews*, 17, 1033-1040.

Olley, J.M., Caitcheon, G.G. and Roberts R.G.,1999. The origin of dose distributions in fluvial sediments, and the prospect of dating single grains from fluvial deposits using -optically stimulated luminescence. *Radiation Measurements,* 30, 207-217.

Olley, J.M., Pietsch, T. and Roberts, R.G., 2004. Optical dating of Holocene sediments from a variety of geomorphic settings using single grains of quartz. *Geomorphology*, 60, 337-358.

Pawley, S.M., Toms, P.S., Armitage, S.J., Rose, J., 2010. Quartz luminescence dating of Anglian Stage fluvial sediments: Comparison of SAR age estimates to the terrace chronology of the Middle Thames valley, UK. *Quaternary Geochronology*, 5, 569-582.

Prescott, J.R. and Hutton, J.T., 1994. Cosmic ray contributions to dose rates for luminescence and ESR dating: large depths and long-term time variations. *Radiation Measurements*, 23, 497-500.

Smith, B.W., Rhodes, E.J., Stokes, S., Spooner, N.A., 1990. The optical dating of sediments using quartz. *Radiation Protection Dosimetry*, 34, 75-78.

Spooner, N.A., 1993. The validity of optical dating based on feldspar. Unpublished D.Phil. thesis, Oxford University.

Stokes, S., Ingram, S., Aitken, M.J, Sirocko, F., Anderson, R. And Leuschner, D., 2003. Alternative chronologies for Late Quaternary (Last Interglacial-Holocene) deep sea sediments via optical dating of silt-sized quartz. Quaternary Science Reviews, 22, 925-941.

Templer, R.H., 1985. The removal of anomalous fading in zircons. *Nuclear Tracks and Radiation Measurements*, 10, 531-537.

Toms, P.S., Hosfield, R.T., Chambers, J.C., Green, C.P. and Marshall, P., 2005. Optical dating of the Broom Palaeolithic sites, Devon and Dorset. English Heritage Centre for Archaeology dating report 16/2005.

Wallinga, J., 2002. Optically stimulated luminescence dating of fluvial deposits: a review. *Boreas* 31, 303-322.

Wintle, A.G., 1973. Anomalous fading of thermoluminescence in mineral samples. *Nature*, 245, 143-144.

Zimmerman, D. W., 1971. Thermoluminescent dating using fine grains from pottery. *Archaeometry*, 13, 29-52.

APPENDIX III: MOLLUSC ANALYSIS

Sarah Wyles
Wessex Archaeology
February 2011

70754 Area 240 East Coast Mollusc Assessments and Analysis

Introduction
Nineteen samples were selected for the assessment of the preserved molluscan remains from four of the vibrocores from the Area 240 area, VC2c, VC7c, VC8c1 and VC9c.

The samples of between 100 and 250 ml were taken from up to five points within each vibrocore (see **Tables 1** and **2**). The samples were processed for the recovery of mollusca and plant remains.

Methods
The samples were processed through wet-sieving through a sieve of 0.25mm mesh sizes. The samples were visually inspected under a x10 to x40 stereo-binocular microscope to determine if molluscs were preserved. Where molluscs were present, preliminary identifications and quantifications of dominant taxa were conducted and are presented below. Habitat preferences follow those described by Kerney (1999) and Barrett and Yonge (1958).

Results
The samples from VC2c and VC9c contained no shells.

A single sample from VC7c contained a range of mollusca. The predominant shells recovered within the sample were those of *Hydrobia*, both *ulvae* and *ventrosa*. There were also a number of shells of cockle (*Cerastoderma* spp.), of the Rissoidae family, of *Scrobicularia/Tellina* type, saddle oyster (*Anomia ephippium*), oyster (*Ostrea edulis*) and a small scallop (*Chlamys* type).

Shells were recovered from three samples within VC8c1. The richest sample was dominated by *Hydrobia*, both *ulvae* and *ventrosa,* and *Valvata* spp*.* There were also a number of shells of *Bithynia* spp., of *Theodoxus fluviatilis*, of cockle, of the Rissoidae family, of oyster, of saddle oyster, of mussel (*Mytilus edulis*), of carpet shell (Venerupidae) and of limpet (*Patella/Diodora* sp.).

A number of shells were also observed within the ostracod samples from these cores. The same range of species was recorded.

Discussion
Hydrobia ulvae and *Hydrobia ventrosa* are typically found on muddy or silty surfaces in estuaries, intertidal mudflats and saltmarshes and are restricted to brackish or salt water. *Scrobicularia* and *Tellina* can inhabit thick mud and muddy sand in estuarine and intertidal conditions, whereas mussels tend to inhabit rocky open shores or rocks within sheltered harbours and estuaries. Limpets and saddle oysters can also exploit this environment. Oysters favour estuaries and shallow coastal regions. Small scallops and carpet shells can be recovered from the middle shore or below while cockles can be found in sandy mud on the middle shore or below. Rissoidae can favour shallow marine environments.

Theodoxus fluviatilis, *Bithynia* spp. and *Valvata* spp. are all fresh-water species which thrive in moving water environments.

The habitats of the molluscs within the assemblages from VC7c and VC8c1 may be indicative of a muddy outer estuarine and shallow marine environment, with a greater fresh-water element in the area of VC8c1.

References

Barrett, J.H. and Yonge, C.M., 1958. *Collins pocket guide to the Sea Shore*, London, Collins

Kerney, M.P, 1999. *Atlas of the Land and Freshwater Molluscs of Britain and Ireland*, Colchester: Harley Book.

Table 1 Shell from VC2c and 7c

Core	VC2c	VC2c	VC2c	VC2c	VC2c	VC7c	VC7c	VC7c	VC7c	VC7c
Depth - Mb OD	28.70-28.80	30.10-30.20	32.40-32.50	32.92-33.02	33.70-33.80	27.99-28.09	28.36-28.46	29.76-29.86	30.72-30.82	31.99-32.09
Size (ML)	250	250	250	100	250	250	250	250	250	250
Flot Size (ML)	80	130	10	5	10	130	150	200	240	175
Species										
Mussel (*Mytilus edulis*)	-	-	-	-	-	-	-	-	-	-
Oyster (*Ostrea edulis*)	-	-	-	-	-	7	-	-	-	-
Saddle Oyster (*Anomia ephippium*)	-	-	-	-	-	10	-	-	-	-
Tellina/Scrobicularia type	-	-	-	-	-	15	-	-	-	-
Carpet shell (Venerupidae)	-	-	-	-	-	-	-	-	-	-
Limpet (*Patella/ Diodora* spp.)	-	-	-	-	-	-	-	-	-	-
Periwinkle (*Littorina* spp.)	-	-	-	-	-	-	-	-	-	-
Cockle (*Cerastoderma* spp.)	-	-	-	-	-	38	-	-	-	-
Rissoides	-	-	-	-	-	25	-	-	-	-
Small scallop (*Chlamys* type)	-	-	-	-	-	1	-	-	-	-
Hydrobia spp.	-	-	-	-	-	151	-	-	-	-
Theodoxus fluviatilis	-	-	-	-	-	-	-	-	-	-
Valvata spp.	-	-	-	-	-	-	-	-	-	-
Bithynia spp	-	-	-	-	-	-	-	-	-	-
Bithynia operculum	-	-	-	-	-	-	-	-	-	-
Total (MNI)	0	0	0	0	0	232	0	0	0	0

Table 2 Shell from VC8c and VC9c

Core	VC8c1	VC8c1	VC8c1	VC8c1	VC9c	VC9c	VC9c	VC9c	VC9c
Depth - Mb OD	31.60-31.70	32.74-32.84	35.25-35.35	36.54-36.64	27.51-27.61	28.64-28.74	30.62-30.72	31.62-31.72	32.06-32.16
Size (ML)	250	250	250	250	250	250	250	250	250
Flot Size (ML)	40	250	230	250	140	150	220	200	5
Species									
Mussel (*Mytilus edulis*)	-	2	-	frags	-	-	-	-	-
Oyster (*Ostrea edulis*)	1	5	-	-	-	-	-	-	-
Saddle Oyster (*Anomia ephippium*)	2	2	-	-	-	-	-	-	-
Tellina/Scrobicularia type	34	-	-	3	-	-	-	-	-
Carpet shell (Venerupidae)	-	1	-	8	-	-	-	-	-
Limpet (*Patella/ Diodora* spp.)	frags	1	-	frags	-	-	-	-	-
Periwinkle (*Littorina* spp.)	-	-	-	1	-	-	-	-	-
Cockle (*Cerastoderma* spp.)	3	30	-	1	-	-	-	-	-
Rissoides	10	13	-	-	-	-	-	-	-
Small scallop (*Chlamys* type)	-	-	-	-	-	-	-	-	-
Hydrobia spp.	4	82	-	-	-	-	-	-	-
Theodoxus fluviatilis	1	22	-	-	-	-	-	-	-
Valvata spp.	1	50	-	-	-	-	-	-	-
Bithynia spp.		37	-	-	-	-	-	-	-
Bithynia operculum	1	+	-	-	-	-	-	-	-
Total (MNI)	37	243	0	10	0	0	0	0	0

APPENDIX IV: WATERLOGGED PLANT ANALYSIS

Dr Chris Stevens
Wessex Archaeology
February 2011

Area 240 East Coast Waterlogged Plant, Charcoal and Insect Assessments

Introduction
Nineteen samples were selected for the assessment of the preserved molluscan remains from four of the vibrocores from the Area 240 area, VC2c, VC7c, VC8c1 and VC9c.

The samples of between 100 and 250 ml were taken from up to five points within each vibrocore (see **Tables 1** and **2**). The samples were processed for the recovery of mollusca and plant remains.

Methods
The samples were processed by wet-sieving using a 0.25mm mesh size. The samples were then visually inspected under a x10 to x40 stereo-binocular microscope to determine if waterlogged plant remains were preserved. Preliminary identifications of dominant or important taxa are noted below, following the nomenclature of Stace (1997).

Results
Very few of the samples contained any waterlogged or organic material, and even fewer had identifiable material. Of those examined only two had potentially identifiable material from them, while a further four had unidentifiable organics. To this we may also add identifiable seeds extracted from the ostracods samples within VC7c and listed below.

VC8c1 31.60-31.70mbOD
The sample from VC8c1 31.60 to 31.70mbOD had several fragments of organics and a few whole seeds of seablite (*Suaeda maritima*), a fragment of bud scale, a seed of white water lily (*Nymphaea alba*), and one of probable pondweed (*Potamogeton* sp.). These samples also had fairly frequent small fragments of charcoal although none were large enough for identification.

White water-lily is a freshwater aquatic, while pondweed is an aquatic that is generally found within fresh-water environments, but some species can be found within brackish water especially within estuarine habitats. Glasswort is a coastal species common within saltmarshes and often found on mudflats. Such an assemblage would be in keeping with rising sea-levels in the early Holocene and coastal/estuarine conditions during the formation of the deposit.

VC7c 28.36-28.46mbOD
Organic material was also recovered in reasonable quantity from a single sample that from VC7c at 28.36-28.46mOD. However, this mainly comprised fragments of stems and rootlets, possibly of brackish or estuarine plants, but equally may come from marine algae (seaweed).

The sample also contained two seeds, seed cases or spores of an unidentified species. The specimens were around 1mm in length and 0.6-0.7mm in width. They had a slight, very fine reticulate cell pattern. They were rounded on one side with a clear “seam” along one side (a low resolution photograph is included below, **Figure 1**). The seeds most closely resemble sea-spurrey (*Spergularia* sp.), but at 1.5mm the seeds are somewhat are larger than most of the species known in the British Isles, which are generally less than 1mm in length.

Figure 1. Photograph of unidentified seeds. The seeds are just under 1.5mm long.

VC7c 27.72 to 28.11mbOD
From this same core in the ostracods samples, but just above this level at between 27.72 to 28.11mbOD were four seeds of tasselweed (*Ruppia* sp.). Single seeds were recovered at 27.72 and 27.91m OD with two seeds from the sample at 28.11m OD. This species is most commonly found in brackish cut off pools on the coast or within lagoon environments where there is both freshwater and marine input.

Organics from Radiocarbon Samples
Additionally, organic material was examined from four further samples only taken for radiocarbon dating at 31.58, 31.69, 31.96 and 32.00mbOD. This material was extremely fragile and in most cases it probably fragmented during processing. However, it was possible to identify it while it was still *in situ* within the core as being from stems of common reed (*Phragmites australis*). Such material no doubt relates to relatively short-lived reed beds, probably within near-coastal or estuarine environments and the formation of the thin peats seen in the core. At this time sea-level was still rising relatively rapidly and the dated remnants of these Phragmites peat beds then provide an indication of sea-level change through time.

No remains of insects or charcoal were seen within the samples.

References
Stace, C., 1997. *New flora of the British Isles* (2nd edition), Cambridge: Cambridge University Press.

APPENDIX V: POLLEN ANALYSIS

Dr Michael Grant
Wessex Archaeology
February 2011

Area 240 Pollen Analysis report

Introduction
Pollen assessment has been undertaken upon pollen samples from four stratified cores taken from features within Area 240. Subsequent analysis has focused upon the three sequences that yielded sufficient pollen concentrations to enable further investigation. This report contains the results of both the assessment and analysis work upon these samples.

Methods
Investigations of the pollen assemblage of stratified sedimentary sequences can provide information on past environments. When a stratified sequence of sediment is investigated, pollen analysis can show how the pollen arriving at the site of deposition has varied over a given time period, and therefore allow interpretations relating to climate change, vegetation history, human activity and the modification of the local environment. Pollen can be preserved in a range of environments, but preservation is principally determined by whether they are anoxic, such as sediments deposited in lakes, fens, mires and buried soils.

Standard preparation procedures were used (Moore et al. 1991). 4cm3 of sediment will be sampled, with a *Lycopodium* spike added to allow the calculation of pollen concentrations. All samples received the following treatment: 20 mls of 10% KOH (80°C for 30 minutes); 20mls of 60% HF (80°C for 120 minutes); 15 mls of acetolysis mix (80°C for 3 minutes); stained in 0.2% aqueous solution of safranin and mounted in silicone oil following dehydration with tert-butyl alcohol.

Pollen counting was done at a magnification of x400 using a Nikon Eclipse E400 / Nikon SE transmitted light microscope. Determinable pollen and spore types were identified to the lowest possible taxonomic level with the aid of a reference collection kept at Wessex Archaeology. The pollen and spore types used are those defined by Bennett (1994; Bennett et al. 1994) with the exceptions given below, with plant nomenclature ordered according to Stace (1997).

The frequent absences of the outer perine (the essential feature for identification) prevented the consistent separation of monoaperturate spores (with the exception of *Polypodium* (polypody) and so these are classed as *Pteropsida* (monolete) indet. (fern spores).

A total land pollen (TLP) sum has been adopted in this study with selected taxa excluded which are likely to be over represented due to their local abundance. These exclusions are *Alnus glutinosa* (alder), Cyperaceae (sedge), obligate aquatics, pteridophytes (includes club moss, horsetails and ferns) and bryophyta (mosses). The desired TLP sum during assessment was 100 grains. Due to many counts falling below this total during the assessment phase, the results are presented as the number of grains of each taxon in Tables 1 to 4. For analysis, a TLP sum of 400 grains was used, though low concentrations in core VC2c meant that a lower count of 200 grains was used in this instance.

Microscopic charcoal analysis was undertaken using the original pollen preparation residues. The method used was adapted from Clark (1982). The amount of charcoal present was quantified by counting a minimum of 200 random fields of view, applied to each slide, and the number of charcoal particles recorded. A minimum of 50 *Lycopodium* spores, added as part

of the original preparation procedure, were also counted enabling the calculation of charcoal concentrations.

Assessment Results
Results of the assessment are given below for each core and the raw pollen counts are shown in Tables 1 to 4.

Core VC2c
Pollen (raw counts) and microscopic charcoal (concentrations) assessment results are shown in Table 1. No pollen was recovered from samples taken at 28.30, 29.10, 29.70, 31.00 and 33.80mb OD and are therefore not discussed below.

Pollen concentrations were highest in the lower deposits and are dominated by *Pinus sylvestris* (pine), Cyperaceae and Poaceae (grasses). Pre-Quaternary spores and indeterminable grain numbers are high indicating some reworked sediment. This may also account for the high amount of poorly preserved *Pinus sylvestris* grains in the samples, many of which were broken. There is also a range of other pollen types which are better preserved in the lower two samples suggesting that not all of the pollen is derived from reworked sediments. Microscopic charcoal is present in all four samples. The pollen concentrations are too low in the upper two samples to enable high pollen counts and therefore little interpretation can be made of the pollen from this section of the core.

Core VC7c
Pollen (raw counts) and microscopic charcoal (concentrations) assessment results are shown in Table 2. No pollen was recovered from samples taken at 30.83, 31.50 and 31.90mb OD and are therefore not discussed below.

Pollen concentrations were highest in the upper deposits and were dominated by *Pinus sylvestris* (pine), *Quercus* (oak) and Poaceae. *Betula* (birch), Chenopodiaceae (fat hen) and Cyperaceae are also present in notable amounts. Pre-Quaternary spores and indeterminable grain numbers are low in comparison to Core VC2c indicating that the amount of reworked sediment is probably low, which is supported by the diverse pollen assemblage. Microscopic charcoal was absent in the two lowest samples, but present in the upper two. The pollen concentrations were too low in the lowest sample to enable high enough pollen counts and therefore little interpretation can be made of the pollen from this section of the core.

Core VC8c1
Pollen (raw counts) and microscopic charcoal (concentrations) assessment results are shown in Table 3. Pollen concentrations were highest in the upper four samples, which are dominated by *Corylus avellana*-type (hazel) with *Pinus sylvestris*, *Ulmus* (elm), *Quercus* (oak), *Betula*, *Alnus glutinosa* and Poaceae. Pre-Quaternary spores and indeterminable grains are present in low concentrations except for the lowest sample. This indicates that the amount of reworked sediment is probably low in the upper samples, which is supported by the diverse pollen assemblage.

Microscopic charcoal was absent in the two lowest samples, but present in the upper four. Pollen concentrations increase towards the top of the sequence, though were too low in the lowest two sample to enable high pollen counts, and therefore little interpretation can be made of the pollen from this section of the core.

Core VC9c
Pollen (raw counts) and microscopic charcoal (concentrations) assessment results are shown in Table 4. Pollen concentrations were low in all samples from this core, with no pollen in the sample from 30.61mb OD. A proportionally high amount of pre-Quaternary spores and indeterminable grains in comparison to identifiable pollen grains are present in

most samples, indicating that the amount of reworked sediment is probably significant and preservation is poor.

Microscopic charcoal was low in most samples. Low pollen concentrations increase towards the top of the sequence, though were too low in the lowest two sample to enable high pollen counts, and therefore little interpretation can be made of the pollen from this section of the core.

Summary of assessment results
Pollen concentrations were sufficient in samples from cores VC7c (27.52 to 28.62mb OD) and VC8c1 (31.59-33.05mb OD) to proceed to full analysis. The samples from core VC7c shows a mixed *Pinus*-*Quercus* woodland with some open ground. The low amounts of *Corylus avellana*-type in this core in comparison to the amount of *Pinus sylvestris* and Quercus may indicate that it is of pre-Holocene date (Pleistocene interglacial). The assemblage in core VC8c1 showing a mixed deciduous woodland and may be Holocene in date.

Although pollen counts nearly reached the desired 100TLP sum in core VC2c, the high proportion of pre-quaternary spores and indeterminable grains indicates that there is a high proportion of reworked sediments and poor pollen preservation. The high amount of *Pinus sylvestris* pollen which was poorly preserved also suggests that this sequence will not provide a representative pollen assemblage. However, given the possible antiquity of the samples from core VC2c, proximity of lithic finds, and no preservation of other environmental proxies in this sediment, further investigations were undertaken.

Insufficient pollen was obtained from core VC9c to make any meaningful assessment of the pollen assemblage reflected in the sequence.

Analysis Results
As stated above, three of the sequences were subject to further investigation. Additional pollen samples were taken from cores VC7c and VC8c1 to produce a higher sampling resolution. Each core is discussed below with reference to previous work from neighbouring offshore areas (Area 254 (Wessex Archaeology 2008) and East Coast Regional Environmental Characterisation project (MALSF 2011)).

Core VC2c
Two pollen samples were subject to analysis from core VC2c, located at 33.00 and 33.24mb OD. The results are shown in **Figure 1**.

Poor pollen preservation and low slide density meant that the TLP count used was only 200 grains. The pollen sequence is dominated by *Pinus sylvestris* and Poaceae, with high amounts of Cyperaceae, *Pteropsida* (monolete) indet., indeterminable grains and pre-Quarternary spores. The preservation of the *Pinus sylvestris* grains in particular was very poor, many of which were highly corroded and broken. Mudie and McCarthy (1994) state that bisaccate pollen are often over-represented in marine sediments as they are fractionated from non-saccate-grains during fluvial transport and can remain buoyant in water for prolonged periods (Traverse and Ginsburg, 1966). Scourse et al. (1998) therefore implore that interpretations of adjacent terrestrial vegetation from near shore marine sequences should therefore accommodate such over-representation of bisaccate taxa. It is therefore likely that these had been transported some distance, possibly by fluvial processes, rather than being local in origin. It is also likely that much of the micro-charcoal has a similar source. In comparison, where present, the grains of Poaceae and Chenopodiaceae were much better preserved possible implying that they were local in origin and represented the local vegetation. This would have probably been an open brackish/ estuarine environment, also supported by the presence of *Plantago maritima* (sea plantain). The single occurrence

of *Dryas octopetala* (mountain avens) may also imply that this is a cold environment. In addition to the high percentages of poorly preserved *Pinus sylvestris*, the abundance of Pteropsida (monolete) indet., Indeterminable grains and pre-Quarternary spores probably imply that much of this sediment is reworked from older sources. Ekman (1998) states that in situations where high frequencies of pre-Quaternary palynomorphs are recording a high influx of reworked sediment, the interpretation of the contemporaneous vegetation is very difficult if not impossible.

Core VC7c
Five pollen samples were subject to analysis from Core VC7c, located between 27.52mb OD and 28.62mb OD. The results are shown in **Figure 2**.

The pollen assemblage is dominated by *Pinus sylvestris*, *Quercus* and Poaceae, with a consistent presence of *Ulmus*, *Corylus avellana*-type, Chenopodiaceae and Cyperaceae. In comparison to core VC2c, the preservation of the *Pinus sylvestris* was very good suggesting that it is unlikely to be derived from reworked material, also supported by the lower presence of pre-Quaternary spores. A number of wetland pollen types are present. The presence of Chenopodiaceae and *Armeria maritima* (thrift) imply some marine/ brackish influence. The abundance of deciduous woodland taxa also implies that this assemblage is likely to be from an inter-glacial/ stadial warm period. Also present are *Vaccinium*-type (bilberries and heath) and *Calluna vulgaris* (heather) which may indicate areas of heath or mire in the local vicinity. The high abundance on *Quercus* in comparison to lower values of *Corylus avellana*-type implies that this is a pre-Holocene sequence. This is confirmed by the OSL samples, with an acceptable (though with strong reservations) date of 96±11 Ka at 27.75-27.85mb OD and an accepted date of 109±11 Ka at 28.62-28.72mb OD. This implies that the sequence is likely to be from Ipswichian (MIS 5e) or Early Devensian (MIS 5d-5b).

A similar assemblage was derived from core VC1c during the Area 254 investigations to the north of the current study area. This showed a much longer pollen assemblage but contained a similar pollen assemblage in Pollen Zone 5 which was dated with OSL to 116.7±11 Ka at the base and a minimum age estimate of (ie older than) 16.6±2.3 Ka at the top (Wessex Archaeology 2008). This sequence was interpreted as Ipswichian (MIS 5e). The close similarity between these two pollen assemblages and their OSL dating would imply that they are contemporary. The high presence of charcoal in the sequence above 27.78mb OD is also a recognised feature of some Ipswichian (Eemian) assemblages (e.g. Daniau *et al*. 2010; Sirocko et al. 2005). Daniau et al. (2010) state that biomass burning was higher during the Holocene and the Eemian than the intervening glacial period, supporting the idea of a strong relationship between global temperature and fire regimes.

Core VC8c1
Seven pollen samples were subject to analysis from core VC8c1, located between 27.52mb OD and 28.62mb OD. The results are shown in **Figure 3**.

The pollen assemblage is dominated by *Quercus* and *Corylus avellana*-type with Pinus sylvestris, Ulmus and Poaceae present throughout. Other notable taxa present include Betula, Alnus glutinosa, Tilia cordata (small-leaved lime), Chenopodiaceae, *Filipendula* (meadowsweet), *Plantago lanceolata* (ribwort plantain) and Cyperaceae. The assemblage implies an area of mix deciduous woodland with some stands of *Pinus sylvestris*. There is a wetland environment present (indicated by taxa such as *Filipendula* and *Sparganium* sp.) which is subject to some marine/ brackish influence, implied by the presence of Chenopodiaceae and *Spergula*-type (sea-spurrey). The presence of Rumex acetosella (sheep's sorrel) and *Plantago lanceolata* in association with peaks in the charcoal record may imply some local disturbance, though this may be in the form of natural burning rather than being necessarily related to anthropogenic activity.

Two radiocarbon dates are available from the upper part of this sequence: 6730-6590 cal. BC (7820±30; SUERC-32233; 31.58mb OD) and 7710-7560 cal. BC (8595±35; SUERC-322234; 32.00mb OD); placing the sequence firmly within the Early Holocene. A similar dated pollen sequences was recovered during the East Coast Regional Environmental Characterisation project (MALSF 2011; core VC18) which had a contemporary radiocarbon date of 7030-6640 cal. BC (7900±35; SUERC-30758; 35.95mb OD), again showing a mixed deciduous woodland with freshwater environs and some marine / brackish influences. A contemporary sequence, albeit with an earlier basal date, has been obtained from a vibrocore situated within Channel B of Area 240, with dates upon the peat between 10710–10280 cal. BC (10470±35; SUERC-11978; 30.80mb OD) and 7530–7350 cal. BC (8370±25; SUERC 11975; 30.05mb OD) (Z. Hazell in preparation).

Summary and Conclusions

Pollen assessment and upon four sequences derived from boreholes in Area 240 has resulted in three sequences being taken to the analysis stage. Combined with the OSL and radiocarbon dating, three distinct periods are covered by these sequences. The age of Core VC2c is unclear but is clearly of Early or Middle Pleistocene in age. Much of the pollen is reworked contributing considerable bias to the pollen assemblage inhibiting its interpretation. However, some of the remaining pollen types may indicate a marine/ brackish environment during cold climatic conditions.

The pollen assemblage from Core VC7c is likely to be of Ipswichian date and shows a strong similarity with the pollen sequence from the top of Core VC1c obtained from Area 254 to the north (Wessex Archaeology 2008). Core VC8c1 is of Early Holocene date and again correlates with other sequences close to the study area. Both sequences show the presence of deciduous woodland within a wetland environment which is influence by marine/ brackish conditions.

Acknowledgements

Pollen assessment and analysis was carried out by Dr Michael Grant, with pollen sample preparation provided at CEESR, Kingston University.

References

Bennett, K.D., 1994. Annotated catalogue of pollen and pteridophyte spore types of the British Isles. Unpublished manuscript, University of Cambridge.

Bennett, K.D., Whittington, G. and Edwards, K.J. 1994. Recent plant nomenclatural changes and pollen morphology in the British Isles. Quaternary Newsletter, 73, 1-6

Clark, R.L., 1982. Point count estimation of charcoal in pollen preparations and thin sections of sediments. Pollen et Spores 24: 523-535.

Daniau, A.-L., Harrison, S.P. and Bartlein, P.J. 2010. Fire regimes during the Last Glacial. Quaternary Science Reviews, 29, 2918-2930.

Ekman, S.R., 1998. Middle Pleistocene pollen biostratigraphy in the central north sea. Quaternary Science Reviews, 17, 931-944.

MASLF 2011. East Coast Regional Environmental Characterisation. Centre for environment, fisheries and aquaculture science open report MEPF 08/04, MASLF, Lowerstoft.

Mudie, P.J. and Aksu, A.E., 1989. Pleistocene palaeoceanography of the northwest Atlantic: planktonic foraminifera, coccolith, dinocyst and pollen records. Abstracts, Third International

Conference on Palaeoceanography, University of Cambridge, UK, September 10-16, 1989, p. 36. Blackwell, London.

Moore, P.D., Webb, J.A. and Collinson, M.E., 1991. Pollen Analysis, 2nd edition. Blackwell Scientific Publications, Oxford.

Scourse, J.D., Ansari, M.H., Wingfield, R.T.R., Harland, R. and Balson, P.S., 1998. A middle pleistocene shallow marine interglacial sequence, inner silver pit, southern north sea: pollen and dinoflagellate cyst stratigraphy and sea-level history. Quaternary Science Reviews, 17, 871-900.

Stace, J., 1997. New flora of the British Isles, 2nd edition. Cambridge University Press, Edition II.

Sirocko, F., Seelos, K., Schaber, K., Rein, B., Dreher, F., Diehl, M., Lehne, R., Jäger, K., Krbetschek, M. and Degering D. 2005. A late Eemian aridity pulse in central Europe during the last glacial inception. Nature, 436, 833-836.

Traverse, A. and Ginsburg, N.G. 1966. Palynology of the surface sediments of Great Bahama Bank, as related to water movement and sedimentation. Marine Geology, 4, 417-459.

Wessex Archaeology, 2008. Seabed Prehistory: Gauging the Effects of Marine Aggregate Dredging. Final Report. Volume IV Great Yarmouth. Unpublished report 57422.34, Wessex Archaeology, Salisbury.

Figures

Figure 1: Pollen Analysis results from Core VC2c
Figure 2: Pollen Analysis results from Core VC7c
Figure 3: Pollen Analysis results from Core VC8c1

Tables

Core	**VC2c**	**VC2c**	**VC2c**	**VC2c**	**VC2c**	**VC2c**	**VC2c**	**VC2c**	**VC2c**
Depth (mb OD)	**28.3***	**29.1***	**29.7***	**31***	**32**	**32.7**	**33**	**33.24**	**33.8***
Pinus sylvestris	-	-	-	-	-	7	43	50	-
Betula	-	-	-	-	1	-	-	-	-
Alnus glutinosa	-	-	-	-	-	4	3	3	-
Carpinus betulus	-	-	-	-	-	1	-	-	-
Corylus avellana-type	-	-	-	-	-	-	2	-	-
Chenopodiaceae	-	-	-	-	1	1	2	1	-
Brassicaceae	-	-	-	-	-	-	4	2	-
Calluna vulgaris	-	-	-	-	4	-	-	-	-
Dryas octopetala	-	-	-	-	-	-	1	2	-
Rosaceae undiff.	-	-	-	-	-	-	-	1	-
Fabaceae undiff.	-	-	-	-	-	-	-	5	-
Apiaceae undiff.	-	-	-	-	-	1	-	-	-
Plantago maritima	-	-	-	-	-	-	-	1	-
Lactuceae undiff.	-	-	-	-	-	-	2	1	-
Artemisia-type	-	-	-	-	-	-	1	-	-
Cyperaceae undiff.	-	-	-	-	1	2	13	14	-
Poaceae undiff.	-	-	-	-	4	9	23	31	-
Pteridium aquilinum	-	-	-	-	-	-	1	-	-
Pteropsida (monolete) indet.	-	-	-	-	-	2	4	6	-
Indeterminable Grains	-	-	-	-	10	9	17	51	-
Pre-Quaternary Spores	-	-	-	-	6	3	11	22	-
TLP SUM	-	-	-	-	10	19	78	94	-
Pollen Concentration (grains cm-3)	-	-	-	-	281	485	9108	20513	-
Microscopic Charcoal Concentration (particles cm-3	-	-	-	-	734	803	18026	11522	-

Table 1: Pollen (raw counts) and microscopic charcoal (concentrations) from Core VC2c. *Insufficient organic content of sediment lead to no pollen residue being produced during sample preparation for assessment.

Core	VC7c	VC7c	VC7c	VC7c	VC7c	VC7c	VC7c
Depth (mb OD)	**27.52**	**28.3**	**28.62**	**29.75**	**30.83***	**31.5***	**31.9***
Picea	2	-	2	-	-	-	-
Pinus sylvestris	64	54	41	-	-	-	-
Ulmus	1	1	-	-	-	-	-
Juglans regia	-	-	-	1	-	-	-
Quercus	30	21	13	2	-	-	-
Betula	8	7	14	3	-	-	-
Alnus glutinosa	1	-	-	-	-	-	-
Fraxinus excelsior	1	-	-	-	-	-	-
Corylus avellana-type	4	-	4	-	-	-	-
Ranunculus acris-type	-	-	1	-	-	-	-
Chenopodiaceae	9	4	8	-	-	-	-
Polygonum	-	-	1	-	-	-	-
Vaccinium-type	1	-	-	-	-	-	-
Calluna vulgaris	1	-	-	-	-	-	-
Filipendula	1	-	-	-	-	-	-
Rubus undiff.	-	2	1	-	-	-	-
Fabaceae undiff.	1	-	-	-	-	-	-
Apiaceae undiff.	1	1	3	-	-	-	-
Plantago coronopus	1	-	-	-	-	-	-
Campanula-type	-	-	1	-	-	-	-
Rubiaceae	-	-	1	-	-	-	-
Cyperaceae undiff.	15	3	6	-	-	-	-
Poaceae undiff.	20	21	13	1	-	-	-
Sparganium erectum	-	-	1	-	-	-	-
Sparganium emersum-type	-	-	1	-	-	-	-
Pteridium aquilinum	2	1	-	-	-	-	-
Pteropsida (monolete) indet.	4	4	22	1	-	-	-
Indeterminable Grains	10	12	3	5	-	-	-
Pre-Quaternary Spores	4	3	2	-	-	-	-
TLP SUM	145	111	103	7	-	-	-
Pollen Concentration (grains cm-3)	16508	14943	3423	108	-	-	-
Microscopic Charcoal Concentration (particles cm-3	2788	2044	0	0	-	-	-

Table 2: Pollen (raw counts) and microscopic charcoal (concentrations) from Core VC7c.. *Insufficient organic content of sediment lead to no pollen residue being produced during sample preparation for assessment.

Core	VC8c1	VC8c1	VC8c1	VC8c1	VC8c1	VC8c1
Depth (mb OD)	**31.59**	**32.06**	**32.26**	**33.05**	**35.2**	**36.53**
Pinus sylvestris	7	23	20	12	1	5
Ulmus	7	11	6	4	-	-
Quercus	19	57	30	29	3	-
Betula	3	4	4	3	-	-
Alnus glutinosa	6	2	4	6	-	2
Tilia cordata	-	-	2	-	-	-
Corylus avellana-type	103	104	71	73	7	-
Hedera helix	1	-	-	2	-	-
Ranunculus acris-type	-	1	-	-	-	-
Urtica dioica	-	-	1	-	-	-
Chenopodiaceae	7	3	7	17	1	-
Spergula-type	-	1	-	1	-	-
Rumex acetosella	1	-	-	-	-	-
Vaccinium-type	-	-	-	-	-	2
Calluna vulgaris	-	-	-	1	-	1
Filipendula	-	-	1	2	-	-
Rosaceae undiff.	1	-	-	-	-	-
Apiaceae undiff.	-	1	-	-	-	-
Plantago coronopus	-	-	-	1	-	-
Plantago lanceolata	1	-	1	-	-	-
Lactuceae undiff.	-	1	-	-	-	1
Solidago virgaurea-type	-	-	1	-	-	-
Cyperaceae undiff.	3	3	1	3	1	-
Poaceae undiff.	11	4	7	17	-	5
Sparganium erectum	1	-	-	2	-	-
Pteridium aquilinum	11	-	2	3	-	-
Pteropsida (monolete) indet.	11	11	10	9	1	3
Bryophyta	-	1	-	-	-	-
Indeterminable Grains	2	0	2	0	3	1
Pre-Quaternary Spores	15	2	9	1	2	47
TLP SUM	161	210	151	162	12	14
Pollen Concentration (grains cm-3)	26373	20088	16261	14207	335	404
Microscopic Charcoal Concentration (particles cm-3	4919	7227	2973	1966	0	0

Table 3: Pollen (raw counts) and microscopic charcoal (concentrations) from Core VC8c1..

Core	VC9c	VC9c	VC9c	VC9c	VC9c	VC9c	VC9c
Depth (mb OD)	**27.5**	**27.9**	**28.75**	**30.61***	**31.61**	**31.8**	**32.05**
Abies	-	-	1	-	-	-	-
Picea	-	-	-	-	-	1	-
Pinus sylvestris	-	-	-	-	2	23	12
Betula	-	-	-	-	-	1	1
Alnus glutinosa	-	-	3	-	-	-	-
Corylus avellana-type	1	-	-	-	-	-	-
Salix	-	-	1	-	-	-	-
Spergula-type	-	-	-	-	-	1	-
Brassicaceae	-	-	-	-	-	-	2
Filipendula	1	-	-	-	-	-	-
Lactuceae undiff.	-	-	-	-	-	-	1
Cyperaceae undiff.	4	-	4	-	1	1	6
Poaceae undiff.	3	2	1	-	3	5	4
Sparganium emersum-type	-	-	-	-	-	-	1
Polypodium	-	-	-	-	-	1	-
Pteropsida (monolete) indet.	-	-	-	-	-	2	-
Indeterminable Grains	0	0	0	-	0	2	1
Pre-Quaternary Spores	-	-	4	-	1	14	35
TLP SUM	5	2	3	-	5	31	20
Pollen Concentration (grains cm-3)	107	245	146	-	213	3220	5018
Microscopic Charcoal Concentration (particles cm-3	37	0	54	-	58	186	3159

Table 4: Pollen (raw counts) and microscopic charcoal (concentrations) from Core VC9c.Insufficient organic content of sediment lead to no pollen residue being produced during sample preparation for assessment.

Figure 1: Area 240, Core VC2C

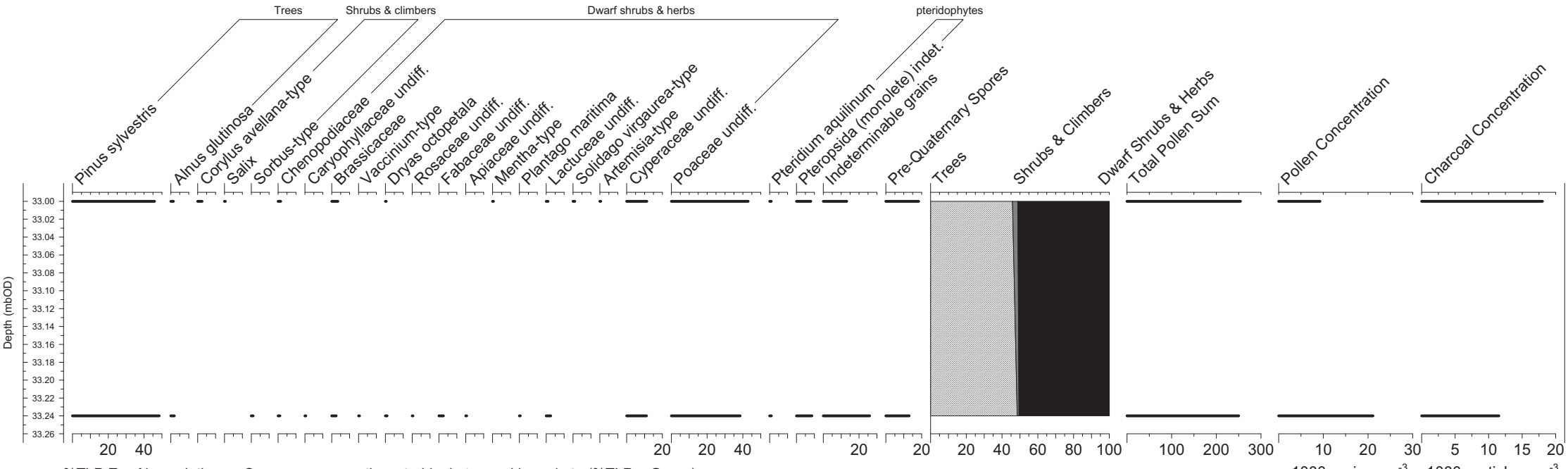

Figure 2: Area 240 Core VC7C

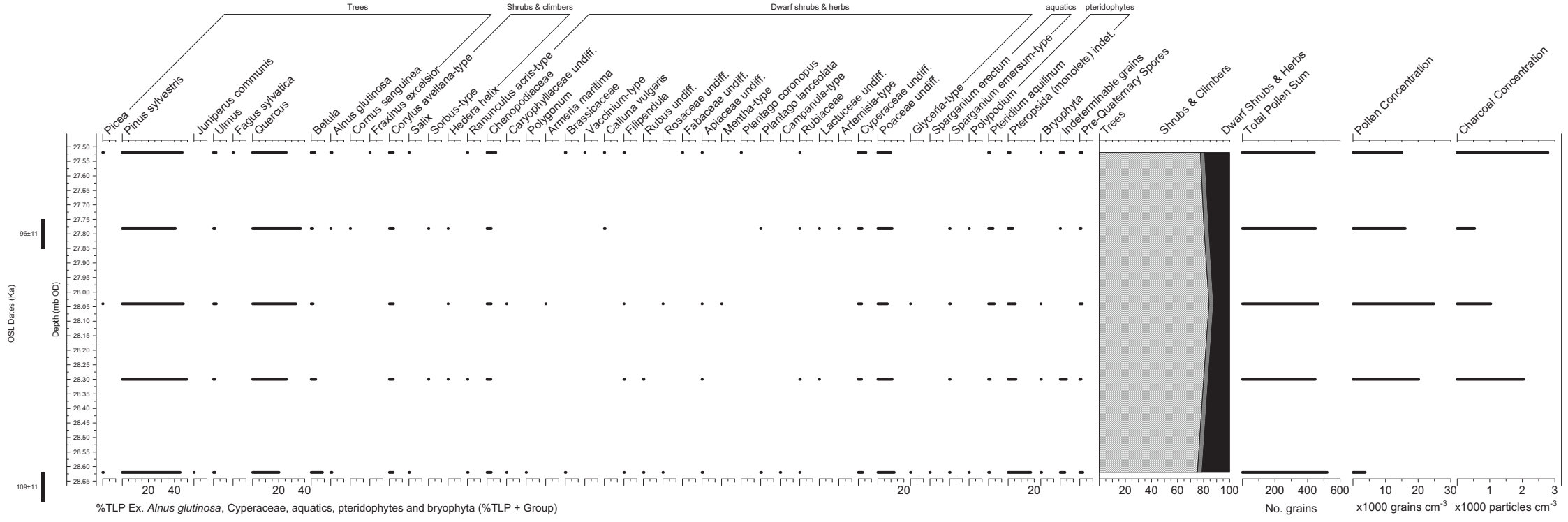

Figure 3: Area 240, Core VC8C

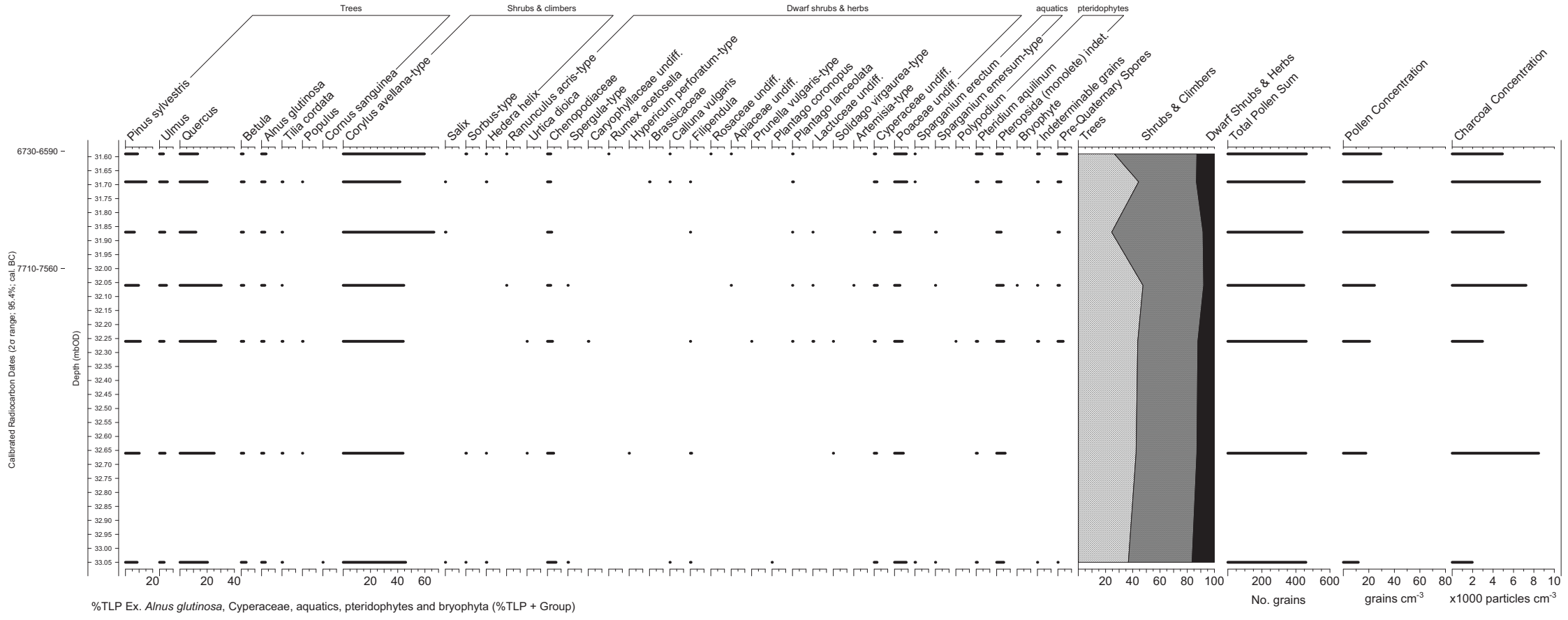

APPENDIX VI: DIATOM ANALYSIS

Diatom assessment of samples from 70754 Seabed Prehistory Area 240

Nigel Cameron, Environmental Change Research Centre,
Department of Geography, University College London,
Pearson Building, Gower Street, London WC1E 6BT

Introduction

Twenty-nine sediment sub-samples from the 70754 Seabed Prehistory Area 240 site (located in the southern North Sea *c.* 12 miles east of Great Yarmouth) have been prepared and assessed for diatoms. Nine samples for diatom evaluation were taken from Vibrocore VC2c, seven samples from VC7c, six samples from VC8c1 and seven samples from VC9c. The purpose of the diatom assessment of the Area 240 sequences is to understand the presence/absence of diatoms within the sequence and the potential of the sediments/samples for further diatom analysis. It is hoped that, if present, the diatoms will inform upon sea level and local environment along with possible comment on chronology, climate and hydrology (Jack Russell pers. comm.). The diatom assessment of each sample takes into account the numbers of diatoms, the state of preservation of the diatom assemblages, species diversity and diatom species environmental preferences.

Methods

Diatom preparation followed standard techniques (Battarbee 1986, Battarbee *et al.* 2001). Two coverslips were made from each sample and fixed in Naphrax for diatom microscopy. A large area of the coverslips on each slide was scanned for diatoms at magnifications of x400 and x1000 under phase contrast illumination.

Diatom floras and taxonomic publications were consulted to assist with diatom identification; these include Hendey (1964), Werff & Huls (1957-1974), Hartley *et al.* (1996) and Krammer & Lange-Bertalot (1986-1991). Diatom species' salinity preferences are discussed in part using the classification data in Denys (1992), Vos & de Wolf (1988, 1993) and the halobian groups of Hustedt (1953, 1957: 199), these salinity groups are summarised as follows:

1. Polyhalobian: >30 g l^{-1}
2. Mesohalobian: 0.2-30 g l^{-1}
3. Oligohalobian - Halophilous: optimum in slightly brackish water
4. Oligohalobian - Indifferent: optimum in freshwater but tolerant of slightly brackish water
5. Halophobous: exclusively freshwater
6. Unknown: taxa of unknown salinity preference.

Results & Discussion

Table 1. Samples from the 70754 Seabed Prehistory Area 240 site selected for diatom evaluation.

Vibrocore	Diatom Sample Number	Sample Depth (m) below OD
VC2c		
	D1	28.30
	D2	29.10
	D3	29.70
	D4	31.00
	D5	32.00
	D6	32.70
	D7	33.00
	D8	33.24
	D9	33.80
VC7c		
	D10	27.52
	D11	28.30
	D12	28.62
	D13	29.75
	D14	30.83
	D15	31.50
	D16	31.90
VC8c1		
	D17	30.59
	D18	32.06
	D19	32.26
	D20	33.05
	D21	35.20
	D22	36.53
VC9c		
	D23	27.50
	D24	27.90
	D25	28.75
	D26	30.61
	D27	31.61
	D28	31.80
	D29	32.05

The diatom sample numbers, sequence number and sample depth are shown in **Table 1** above. The results of the diatom evaluation for the Area 240 samples are summarised in **Table 2** and the diatom species recorded are shown in **Table 3** along with their halobian classifications.

Table 2. Summary of diatom evaluation results for 70754 Seabed Prehistory Area 240 (+ present, - absent, mod – moderately high, fw – freshwater, bk – brackish, mar – marine)

Diatom Sample No.	Diatoms	Diatom numbers	Quality of preservation	Diversity	Assemblage type	Potential for % count
D1	-	-	-	-	-	none
D2	-	-	-	-	-	none
D3	-	-	-	-	-	none
D4	-	-	-	-	-	none
D5	-	-	-	-	-	none
D6	-	-	-	-	-	none
D7	-	-	-	-	-	none
D8	-	-	-	-	-	none
D9	-	-	-	-	-	none
D10	-	-	-	-	-	none
D11	-	-	-	-	-	none
D12	-	-	-	-	-	none
D13	-	-	-	-	-	none
D14	-	-	-	-	-	none
D15	-	-	-	-	-	none
D16	-	-	-	-	-	none
D17	+	very low	very poor	low/mod	mar bk fw	none
D18	+	low	poor to mod	mod	mar bk fw	none
D19	+	very low	very poor	low	mar bk	none
D20	+	very low	very poor	very low	mar bk	none
D21	-	-	-	-	-	none
D22	-	-	-	-	-	none
D23	-	-	-	-	-	none
D24	-	-	-	-	-	none
D25	-	-	-	-	-	none
D26	-	-	-	-	-	none
D27	-	-	-	-	-	none
D28	-	-	-	-	-	none
D29	-	-	-	-	-	none

Vibrocore VC2c

Diatoms are absent from the nine sub samples (D1-D9) assessed from VC2c. This may reflect unfavourable conditions for diatom silica preservation (Flower 1993, Ryves *et al.* 2001). It is not therefore possible to comment on the salinity or other aspects of the aquatic environment.

Vibrocore VC7c

Diatoms are absent from the seven sub samples (D10-D16) assessed from VC7c.

Vibrocore VC8c1

Diatoms are absent from the two lower samples (D21 and D22) in VC8c1. Poorly preserved diatom assemblages are present in the top four samples (D17-D20) from VC8c1 (Table 2). The diatom numbers in these four samples is low or very low and the quality of preservation is generally very poor with most diatoms only represented by small fragments. Diatom species diversity varies from moderate to very low. As a result of the poor quality of diatom preservation there is no potential for percentage diatom counting of the four diatomaceous

samples, however, the diatom assemblages are consistent with marine-brackish environments and are discussed below.

The preserved diatom assemblages lie between 33.05 m below OD and 30.59 m below OD in VC8c1. The sediment lithologies in this part of the sequence have been interpreted as shallow marine, outer estuary and mudflat (Jack Russell pers. comm.). Consistent with marine conditions, the diatomaceous samples contain polyhalobous, planktonic taxa such as *Paralia sulcata, Podosira stelligera*, *Triceratium favus, Auliscus sculptus* and the marine-brackish diatom *Actinoptychus undulatus*. Non-planktonic polyhalobous and polyhalobous to mesohalobous diatoms present in the VC8c1 assemblages include *Grammatophora* sp. *Rhaphoneis amphiceros, Dimeregramma minor, Cocconeis scutellum* and the benthic diatoms *Trachyneis aspera* and *Lyrella atlantica*.

The brackish-marine diatoms present are, with the exception of *Cyclotella striata* (an estuarine planktonic diatom), benthic diatoms or diatoms that grow attached to submerged surfaces (e.g. *Synedra gaillonii*). These mesohalobous diatoms present include benthic species such as *Catenula adhaerans, Diploneis didyma, Nitzschia navicularis, Nitzschia granulata, Nitzschia hungarica* and *Nitzschia punctata*

In the top two samples from VC8c1 there are very low numbers of freshwater, oligohalobous indifferent taxa. These diatoms include the epiphytic freshwater, oligohalobous indifferent species *Cocconeis placentula* and the oligohalobous indifferent to halophilous epiphytic genus *Epithemia*, *Fragilaria construens* and (possibly) *Fragilaria pinnata*. These *Fragilaria* taxa have optimal growth in freshwater but have wide salinity tolerance.

The dominance of polyhalobous and mesohalobous species and scarcity of oligohalobous indifferent and halophilous diatoms in samples D17-D20 reflect marine-brackish sedimentary environments. The components of mesohalobous benthic and attached diatoms are consistent with shallow water marine conditions. Benthic mesohalobous taxa such as *Navicula navicularis, Nitzschia punctata, Nitzschia granulata* and *Diploneis didyma* are typical of tidal mudflats.

Vibrocore VC9c

Diatoms are absent from the seven sub samples (D23-D29) assessed from VC9c.

Table 3: The diatom species recoded in each core with their halobian classifications

Diatom Taxon/Laboratory Sample Number	D17	D18	D19	D20
Polyhalobous				
Auliscus sculptus	-	-	-	1
Coscinodiscus sp.	1	-	cf	-
Dimeregramma minor	1	1	-	1
Grammatophora sp.	2	1	1	-
Lyrella atlantica	-	1	-	-
Paralia sulcata	1	2	1	1
Podosira stelligera	1	-	cf	1
Rhaphoneis amphiceros	-	1	-	-
Trachyneis aspera	-	1	-	-
Triceratium favus	1	-	-	-
Polyhalobous to Mesohalobous				
Actinoptychus undulatus	-	1	1	1
Cocconeis scutellum	-	1	1	1
Synedra gaillonii	1	-	cf	1
Mesohalobous				
Campylodiscus sp.	-	-	1	-
Catenula adhaerans	-	1	-	-
Cyclotella striata	-	-	-	1
Diploneis didyma	-	-	1	-
Nitzschia punctata	-	2	-	-
Nitzschia granulata	1	-	-	-
Nitzschia hungarica	-	-	1	-
Nitzschia navicularis	1	cf	-	-
Synedra tabulata (fasciculata)	1	1	-	-
Oligohalobous Indifferent				
Cocconeis placentula	-	1	-	-
Epithemia sp.	1	-	-	-
Fragilaria construens	-	1	-	-
Fragilaria pinnata	-	cf	-	-
Unknown Salinity Group				
Achnanthes sp.	1	-	-	-
Diploneis sp.	-	1	1	1
Fragilaria sp.	-	1	-	-
Inderminate centric fragments	1	1	1	1
Inderminate pennate fragments	2	2	1	2
Nitzschia sp.	-	-	-	1
Surirella sp.	1	-	-	-
Synedra sp.	1	1	-	1
Thalassiosira sp.	-	1	-	-
Unknown diatom fragment	1	1	1	1
Unknown naviculaceae	-	-	-	1

Conclusions

1. Diatoms are absent from the samples assessed from VC2c, VC7c and VC9c, and are also absent from lower two samples in VC8c1. Diatom assemblages are present in the top four samples in VC8c1, however the quality of preservation is poor and there is no potential for percentage diatom counting of these samples.

2. In the top four samples from VC8c1 in which diatoms are present the assemblages consistently reflect marine-brackish habitats. There is a mixture of coastal plankton and shallow water non-planktonic diatoms, including benthic and attached polyhalobous to mesohalobous taxa. In the top two samples of VC8c1 there are a very small number of oligohalobous indifferent and halophilous diatoms. These are often found in coastal and estuarine diatom assemblages as a result of the inwash of diatoms from freshwater habitats.

Acknowledgements

Thanks to Jack Russell of Wessex Archaeology for providing the samples for diatom assessment and for background information on the Seabed Prehistory Area 240 site.

References

Battarbee, R.W., 1986. Diatom analysis. In: Berglund, B.E. (ed) Handbook of Holocene Palaeoecology and Palaeohydrology. John Wiley, Chichester, 527-570.

Battarbee, R.W., Jones, V.J., Flower, R.J., Cameron, N.G., Bennion, H.B., Carvalho, L. and Juggins, S., 2001. Diatoms. In (J.P. Smol and H.J.B. Birks eds.), Tracking Environmental Change Using Lake Sediments Volume 3: Terrestrial, Algal, and Siliceous Indicators, 155-202. Dordrecht: Kluwer Academic Publishers.

Denys, L., 1992. *A check list of the diatoms in the Holocene deposits of the Western Belgian Coastal Plain with a survey of their apparent ecological requirements: I. Introduction, ecological code and complete list.* Service Geologique de Belgique. Professional Paper No. 246. pp. 41.

Flower, R.J., 1993. Diatom preservation: experiments and observations on dissolution and breakage in modern and fossil material. *Hydrobiologia 269/270*: 473-484.

Ryves, D. B., Juggins, S., Fritz, S. C. and Battarbee, R. W., 2001. Experimental diatom dissolution and the quantification of microfossil preservation in sediments. *Palaeogeography, Palaeoclimatology, Palaeoecology*, 172, 99-113

Hartley, B., H.G. Barber, J.R. Carter and Sims, P.A., 1996. *An Atlas of British Diatoms.* Biopress Limited. Bristol. pp. 601.

Hendey, N.I., 1964. An Introductory Account of the Smaller Algae of British Coastal Waters. Part V. Bacillariophyceae (Diatoms). Ministry of Agriculture Fisheries and Food, Series IV. pp. 317.

Hustedt, F., 1953. Die Systematik der Diatomeen in ihren Beziehungen zur Geologie und Okologie nebst einer Revision des Halobien-systems. *Sv. Bot. Tidskr.*, 47: 509-519.

Hustedt, F., 1957. Die Diatomeenflora des Fluss-systems der Weser im Gebiet der Hansestadt Bremen. *Ab. naturw. Ver. Bremen* 34, 181-440.

Krammer, K. and Lange-Bertalot H., 1986-1991. *Bacillariophyceae.* Gustav Fisher Verlag, Stuttgart.

Vos, P.C. & H. de Wolf, 1988. Methodological aspects of palaeoecological diatom research in coastal areas of the Netherlands. *Geologie en Mijnbouw* 67: 31-40

Vos, P.C. and de Wolf, H. 1993. Diatoms as a tool for reconstructing sedimentary environments in coastal wetlands; methodological aspects. *Hydrobiologia* 269/270: 285-296

Werff, A. Van Der and Huls, H., 1957-1974. *Diatomeenflora van Nederland*, 10 volumes

APPENDIX VII: FORAMINIFERA AND OSTRACOD ANALYSIS

70754 Seabed Prehistory, Area 240 Foraminifera and Ostracod analysis

Jack Russell
Wessex Archaeology
February 2011

Introduction
Forty-three sediment sub-samples taken from four vibrocores, VC2c, VC7c, VC8c1 and VC9c located *c.*11km east of Great Yarmouth in the aggregate dredging Area 240, Southern North Sea have been investigated for the presence and environmental significance of their microfaunal contents, predominantly ostracods and foraminifera. The retrieved sediments are gravels sands, silts and clays from within channel systems thought to be associated with prehistoric finds from the area. Ostracods and foraminifera occurred in twenty-five of the samples. Other plant and animal remains were also recovered from the samples a note of which has been made here. These sediments had been subject to an assessment of foraminifera and ostracods (Wessex Archaeology 2010). The results of the assessment indicated sediments within vibrocores VC7c, VC8c1 and VC9c as containing foraminifera and/or ostracod faunas worthy of further analyses, the results of which are presented here.

Method
Sediment samples of *c.*25g were disaggregated in a weak solution of Hydrogen Peroxide and water, then wet sieved through a 63µm sieve. The sediment was dried and sieved through 500µm, 250µm, 125µm sieves. Microfossils were picked out under 10-60x magnification and transmitted and incident light using a Vickers binocular microscope. Where possible a minimum of one hundred specimens per sample were picked out and kept in card slides. Identification and environmental interpretation of ostracods follows Athersuch *et al*. (1989) and Meisch (2000) and of foraminifera (Murray 1976, 2000).

Results
Abundance of microfaunal remains within the samples is summarised in **Tables 1** to **4**. Abundance of ostracods was varied and where present, the preservation was in general very good. Eighteen of the samples contained ostracods. Foraminifera were proportionally more abundant that ostracods and generally well preserved. Twenty-five of the samples contained foraminifera.

VC2c
Nine samples were assessed at 33.8, 33.24, 33.00, 32.70, 32.00, 31.00, 29.70, 29.10 and 28.30mbOD. None of the samples contained foraminifera or ostracods and as such were not further investigated in this analysis phase.

Other remains within these samples included charcoal, plant remains and coal which were recovered in small amounts (**Table 1**).

VC7c
Eleven samples were investigated at 31.90, 31.50, 30.83, 29.75, 28.62, 28.36, 28.30, 28.11, 27.72, 27.91 and 27.52mbOD. Foraminifera and ostracods were recovered from the upper samples only at 28.36, 28.30, 28.11, 27.72, 27.91 and 27.52mbOD (**Table 2**).

The ostracods recovered were dominated by brackish forms including *Cyprideis torosa*, *Loxoconcha elliptica*, *Loxoconcha rhomboidea* and *Leptocythere psammophila*. Occasional occurrences of *Aurila convexa*, *Carinocythereis carinata, Cytheridea littoralis, Paracytherois flexuosa* and *Propontocypris trigonella* were also noted.

At 28.30 and 27.72mbOD *Cyprideis torosa* was the dominant taxon, and was very abundant in the sample at 28.30mbOD with several hundred specimens noted which included whole carapaces and adult and juvenile forms. A small number of the noded form of *Cyprideis torosa* was also recorded from this sample.

At 28.11, 27.91 and 27.52mbOD *Loxoconcha rhomboidea* was the most numerous taxon recovered although significant numbers of *Loxoconcha elliptica* and *Cyprideis torosa* were also recovered. These three species were well preserved and represented by whole carapaces and instar stages.

The foraminifera from these samples (28.30, 28.11, 27.72, 27.91 and 27.52mbOD) were present in relatively low numbers and generally well preserved. Variants of the species *Ammonia beccarii* were present in all of the samples. Species of the genus *Elphidium* (were present in these samples except at 27.91mbOD). Rotaliid foraminifera including *Haynesina germanica*, *Jadammina macrescens* and Miliolids were also present at these levels. Miliolids including *Milammina fusca*, *Miliolinella subrotundata*, *Quinqueloculina bicornis* var. *angulata* and *Quinqueloculina cliarensis*.

The lower samples were generally devoid of environmental remains. Coal was present in the samples at 31.90, 30.83 and 29.75mbOD. Unidentified plant material and wood was present in the samples at 28.62 and 28.30mbOD. Sponge spicules, a crustacean claw and various marine molluscs were recovered from the samples at 28.30 and 27.52mbOD.

VC8c1
Thirteen samples were investigated for ostracods and foraminifera at 36.53, 35.20, 33.65, 33.05, 32.78, 32.52, 32.36, 32.06, 31.93, 31.81, 31.69 and 31.59mbOD (**Table 3**).

No ostracods were recovered from the samples at 36.53 and 33.65mbOD. At 35.20mbOD a small assemblage including one united carapace and one juvenile valve of the species *Cyprideis torosa*, one adult valve of the species of the ostracod *Loxoconcha elliptica* was recovered. At 33.05mbOD a small assemblage of ostracods incuding one Candoniid, *Cyprideis torosa* and *Leptocythere psammophila* was recovered. At 32.78 *Cyprideis torosa*, *Heterocytheris albumaculata*, *Hirschmannia viridis*, *Loxoconcha elliptica* and *Loxocncha rhomboidea* were recovered. At 32.52mbOD a similar but more abundant fauna was recovered including whole carapaces and instar stages of *Cyprideis torosa*, *Heterocytheris albumaculata*, *Hirschmannia viridis and Loxoconcha elliptica* were recovered. Additionally some specimens of *Cytherura*, *Hemicythere* and *Propontocypris* were recovered at 32.52mbOD.

Above this at 32.26mbOD ostracods were more abundant dominated by adults, juveniles and whole carapaces of the ostracods *Cyprideis torosa*, *Lepyocythere psammophila* and *Loxoconcha elliptica*. At 32.06mbOD the ostracods recorded were dominated by the species including *Cyprideis torosa* and *Loxoconcha elliptica*. Other species included *Loxoconcha rhomboidea*, *Hirschmannia viridis* and *Propontocypris trigonella*. Significant numbers of *Loxoconcha rhomboidea* were also noted within the sample. At 32.00, 31.93, 31.81 and 31.69mbOD similar ostracod faunas were recovered dominated by *Heterocythereis albumaculata* including significant numbers of *Loxoconcha elliptica* and *Hirschmannia viridis* also present. The uppermost sample at 31.59mbOD contained a diverse assemblage of ostracods dominated by *Cytherura gibba*, *Hirschmannia viridis* and *Loxoconcha elliptica*.

Foraminifera were sparse in the lower samples within VC8c1. At 36.53mbOD some worn and fossilised Rotaliid forams, *Protelphidium orbiculare/Elphidiella* were recovered.

Above this at 35.20mbOD a small assemblage of foraminifera including variants of the species of *Ammonia beccarii* and Miliolids were recovered. At 33.65 mbOD a very small assemblage of rotaliid foraminifera was recovered. At 33.05, 32.78 and 32.52mOD foraminifera were more abundant dominated by variants of *Ammonia beccarii.* Other species present included *Haynesina germanica*, *Jadammina macrescens*, Miliolids and species of the genus *Elphidium*.

At 32.26mbOD a similar *Ammonia beccarii* dominated assemblage was recovered with additional *Jadammina macrescens* and Miliolids present.

At 32.06, 32.00, 31.93 and 31.81mbOD the foraminiferal assemblages were numerically dominated by variants of *Ammonia becarrii*. Species of the genus *Elphidium* were also common as were Miliolids. At 32.00 mbOD the variants of *Ammonia becarrii* were notably small, recovered from the in the sub 250µm fractions.

At 31.69mbOD similar numbers of *Ammonia becarrii* were recovered to the samples immediately below however these were dominated by the variant *Ammonia batavus*. Another notable difference in this sample was the increase in numbers of species of *Elphidium* (*Elphidium crispum*, *Elphidium macellum*) and Miliolids (*Miliolinella subrotundata*).

The uppermost sample at 31.69mbOD contained a very high abundance of *Ammonia becarii* variants with noteable numbers of species of *Elphidium* (*Elphidium incertum*, *Elphidium macellum*, *Elphidium williamsoni* and other species such as *Haynesina germanica* and *Brizalina variabilis.*

Other remains in the samples included molluscs (*Cerastoderma edule*, *Mytilus edulis*, *Ostrea edulis*, *Theodoxius fluviatilis*, *Piscidium*, *Bithynia*, Rissoids, Planorbids and Tellin type bivalves, barnacle plates, sponge spicules, echinoids and calcareous tubes. Plant remains recovered included charcoal (at 31.59mbOD), charophyte oogonium (33.05mbOD), a radiate diatom (32.06mbOD) and an unidentified seed at 31.59mbOD.

VC9c
Eleven samples were investigated for foraminifera and ostracods from VC9c at 32.50, 32.05, 31.90, 31.98, 31.83, 31.80, 31.61, 30.61, 28.75, 27.9 and 27.50mbOD (**Table 4**).

Ostracods were absent from all of the samples in VC9c except one ostracod valve of the species *Heterocythereis albomaculata* which was recovered at 31.80mbOD.

Foraminifera were also sparse within the samples. No foraminifera were recovered from the samples at 31.61, 30.61, 28.75, 27.9 and 27.50mbOD.

At 32.50, 32.05, 31.90, 31.98, 31.83 and 31.80mbOD similar foraminiferal assemblages were recovered species recovered comprising *Ammonia beccarii*, *Elphidiella* cf. *hannai*, *Elphidium* cf. *arcticum*, *Lagena* sp., *Lamarckina haliotidea Protelphidium orbiculare* and *Uvigerina/Buliminella*. Most of the specimens were very worn and damaged precluding confident taxonomic work

Other remains recovered within the samples included barnacle plates, plant remains, radiate diatoms, coal and wood.

Discussion

VC2c
Little can be said about the samples from this vibrocore regarding their ostracod and foraminiferal content. The other remains with the samples are of interest including plants and

particularly charcoal at 32.00mbOD which indicate a proximity to terrestrial and potentially inhabited environments. The lack of molluscs within the samples is also of note. Shallow marine deposits of sand identified in other cores are noted for their molluscan content (and foraminifera and ostracods). Within this core no marine environmental remains were recorded which may indicate that the sediments have formed within a freshwater possibly glaciofluvial alluvial outwash environment.

VC7c

The lower samples within this vibrocore lacked environmental remains (at 31.90, 31.50, 30.83, 29.75 and 28.62mbOD), similar to the samples investigated in VC2c and might indicate deposition in a glaciofluvial alluvial outwash environment. The sands and gravels were noted to be predominantly quartzose. The upper samples (at 28.36, 28.30, 28.11, 27.72, 27.91 and 27.52mbOD) contain good faunas of marine and brackish ostracods including *Cyprideis torosa* which dominates the samples at 28.30mbOD and 27.72mbOD. Although *Cyprideis torosa* is an euryhaline taxon that can occur in freshwater to hypersaline conditions, it's mass development is usually associated with a substrate consisting of soft mud and organic detritus in brackish salinities, between 2 and 16.5‰ (Meisch 2000). Most of the specimens recorded were the smooth form however at 28.30mbOD some noded forms were recorded. The node sites are genetically controlled however their development is a physiological response to external conditions and it appears that the nodes more frequently occur in low salinities 2-5‰ (Boomer 2001). At this level an estuarine environment consisting of brackish tidal creeks is interpreted.

Loxoconcha rhomboidea which dominated the samples at 28.11, 27.91 and 27.52mbOD is a shallow marine species which also colonises the mouths of estuaries (Athersuch *et al.* 1989). Given *Cyprideis torosa* and *Locxoconcha elliptica* were also present in high numbers in these samples, represented by both adult and instar stages, it is likely based on the ostracod faunas that an estuary mouth environment for the samples at 28.11, 27.91, 27.72, and 27.52mbOD. Occasional occurrences of shallow marine taxa such as *Aurila convexa*, *Carinocythereis carinata*, *Cytheridea littoralis*, *Paracytherois flexuosa*, and *Propontocypris trigonella* were recorded at these levels. At 27.72 *Cyprideis torosa* and *Locxoconcha elliptica* were more dominant indicating a slightly more brackish than marine influence at this level.

The foraminiferal assemblages within the samples were small and contained a mix of saltmarsh, estuarine and shallow marine forms indicating some reworking and transport of foraminifera within these sediments. As such is not considered possible to make any definite ecological interpretations based on the foraminifera alone. Shallow marine forms were however predominant within the samples, particularly the sample at 27.52mbOD which contained large numbers of Miliolid foraminifera (*Miliolinella subrotundata*, *Quinqueloculina bicornis* var. *angulata* and *Quinqueloculina cliarensis*).

Other remains within the samples including molluscs indicative of estuarine and brackish water environments included the molluscs *Cerastoderma* spp., *Ostrea edulis* and *Hydrobia* sp..

VC8c1

Throughout this core the samples which contained faunal material were indicative of shallow marine, estuarine and brackish environment. The basal sample at 36.53mbOD included some fossilised foraminifera of the genera *Elphidiella/Protelphidium*. These types of foraminifera are known from Pleistocene pre-Anglian cold estuarine environments (Funnell 1989), although are possibly reworked within these sediments. Similar types of foraminifera were recovered from the samples in VC9c. The molluscan assemblage from this level also contains molluscs indicative of marine environments and whilst the foraminifera may be redeposited, a shallow marine depositional environment is likely.

A number of the faunas recovered from the samples within vibrocore VC8c1 contained species indicative of a wide variety of environments ranging from freshwater to marine within the same sample. Rather than reworking of material, it is considered likely that large numbers (particularly of foraminifera) have been transported by tidal and marine currents, and also freshwater elements have been transported from upstream to what were predominantly brackish water environments. The taphonomy of some of the marine and freshwater species confirms this in some cases. In order to identifiy the depositional environment at the sample levels, the ostracods are particularly useful as the preservation of faunas including whole carapaces (united valves), juvenile and adult stages of on species is a good indication that the ostracods have not been transported.

Above this level a sparse assemblage of shallow marine and estuarine foraminifera and ostracods at 35.20mbOD and 33.65mbOD is superceeded by more abundant remains of foraminifera and ostracods in the samples at 33.05, 32.78, 32.52mbOD. The foraminiferal assemblages at these levels are dominated by estuarine and shallow marine forms including variants of *Ammonia becarii*. The variant *Ammonia batavus* with the umbilical boss, which are found more usually in inner shelf and shallow marine environments in contrast to the other variants (*Ammonia aberdoveyensis*, *Ammonia limnetes* and *Ammonia tepida*) which are found more commonly in estuaries and lagoons. Types of Miliolids, *Haynesina germanica* and species of *Elphidium* were also common in these three samples. Amongst other remains within these samples, molluscs were frequent including brackish and marine forms (*Cerastoderma* spp. and *Ostrea edulis*) and also some presumably transported freshwater molluscs including *Bithynia* (opercula and apices) and *Theodoxius fluviatilis*. *Theodoxius fluviatilis* is however noted to tolerate slightly saline waters. It is however the ostracods which are able to throw most light upon some quite mixed assemblages. At 33.05mbOD, a small ostracod assemblage included a number of whole carapaces of *Leptocythere psammophila* which has an ecological preference for estuaries with a sandy substrate (Athersuch *et al.* 1989). Above this, at 32.78mbOD ostracods were present although not as united carapaces or with juvenile and adults stages At 32.52mbOD *Cyprideis torosa* and *Loxoconcha elliptica* were recovered in high numbers including whole carapaces, adult and instar stages giving a clear indication of estuarine and brackish conditions at this level.

Cyprideis torosa was recorded in increasing numbers with a high abundance (including whole carapaces, adults and instars) noted at 32.26mbOD. *Loxoconcha elliptica* and *Leptocythere psammophila* were also recorded at this level. As noted above, although *Cyprideis torosa* is an euryhaline taxon that can occur in freshwater to hypersaline conditions, it's mass development is usually associated with a substrate consisting of soft mud and organic detritus in brackish salinities, between 2 and 16.5‰ (Meisch 2000). Within this sample some marine and brackish foraminifera were recorded (variants of *Ammonia becarrii and* Miliolids) and also some marine, brackish and presumably transported freshwater (*Bithynia*, *Piscidium* and *Theodoxius fluviatilis*) molluscs. These faunal remains indicative of freshwater and marine input into the sediments is of interest as they suggest potential fluctuation in salinitiy which is indicated by a fauna dominated by *Cyprideis torosa*.

At 32.00m the ostracod fauna is dominated by whole carapaces, adults and instars of *Hirschmannia* viridis and *Heterocythereis albumaculata* and to a lesser extent *Loxococha rhomboidea*. *Hirschmannia viridis* weed rich littoral fringes of marine and brackish water. Loxoconcha *rhomboidea* and *Heterocythereis albomaculata* prefer littoral and shallow sublittoral fringes marine and outer estuarine environments. Given the large number of *Phragmites* reeds noted within this sample forming peaty layers, a vegetated fringe of a saltmarsh within an estuarine environment is interpreted. Other species within this sample confirm this interpretation, including the foraminifera *Haynesina germanica* and the estuarine and brackish variants of *Ammonia becarrii* were present within the sample although most were noted to be very small and underdeveloped, which may be an indication of transportation.

At 31.93, 31.81, the occurrence of *Hirshcmannia viridis, Heterocythereis albomaculata* with *Loxoconcha elliptica* and *Leptocythere pelluciada* continues indicating a continuation of this shallow littoral environment on the fringes of an estuary. A marine contact is noted with species such as the ostracod *Semicytherura striata* and the foraminifera *Lamarckina haliotidea* being recorded.

By 31.69mbOD *Heterocythereis albumaculata and Leptocythere pellucida* dominate the assemblage, with the latter more indicative of marine sublittoral environments. Foraminifera recovered from this sample also indicate an increasing marine influence. The numerically most dominant species recovered was *Ammonia becarrii* with the variant *Ammonia batavus* being most common, indicative of outer estuarine and marine environments. Large numbers of species of *Elphidium* were also recorded including large numbers of *Elphidium crispum* and *Elphidium macellum*, both indicative of estuary mouths and marine sublittoral environments.

The uppermost sample at 31.59mbOD was dominated by the ostracods indicative of littoral, sublittoral, marine and estuarine environments including *Hirshcmannia viridis*, *Heterocythereis albomaculata* with *Cytherura gibba.* The foraminifera at this level were mixed although also dominated by estuarine and marine forms including species of *Elphidium and Miliolids.*

Significant amounts of charcoal at 31.59mbOD. This charcoal might be indicative of occupation in the vicinity. The freshwater molluscs were noted to be worn and probably reworked in these samples.

VC9c
The samples within VC9c at 32.50, 32.05, 31.90, 31.98, 31.83 and 31.80mbOD contained foraminifera indicative of shallow marine and outer estuarine environments. Whilst it was difficult to ascribe some of the specimens to species level, the predominantly *Elphidium* (*Elphidium* cf. *arcticum* and *Protelphidium orciculare*) and *Elphidiella* (*Elphidiella* cf. *hannai*) are usually associated with pre-Anglian cold stages of the Early Pleistocene (Funnell 1989) similar to the assemblage recovered at the base of VC8c1. It is possible that these foraminifera are reworked within these sediments.

The upper samples within VC9c at 31.61, 30.61, 28.75, 27.9 and 27.50mbOD which contained no foraminifera or ostracods however wood (30.61mbOD) and plant remains (27.90mbOD) recovered are indicative of proximal terrestrial environments.

Dating, sea level and environment

The productive samples within the sediments investigated here for foraminifera and ostracods all indicate brackish and shallow marine environments. The small numbers of freshwater molluscs noted within the samples within VC8c1 are clearly reworked and transported. The lack of foraminifera and ostracods at the top of VC9c and in VC2c may be due to deposition in non-marine environments.

Unfortunately no ostracods were identified in any of the cores which have restricted Pleistocene stratigraphical ranges (Whittaker and Horne 2009). The ostracods recovered were however of much interest due to their value as palaeoenvironmental proxies.

Foraminifera, which were more common within the sediments do not have useful Pleistocene stratigraphical ranges based upon evolution and extinction, however faunal associations which are environmentally controlled have been recorded in the North Sea region (Funnell 1989). From the foraminiferal assemblages, a group of possible pre-Anglian cold stage

foraminifera can be identified, at the base of core VC8c1 (36.53mbOD) and the base of core VC9c (at 32.50, 32.05, 31.98, 31.90, 31.83, and 31.80mbOD). It is however possible that these specimens are reworked as they are very worn. The results of stratigraphic integration between geophysical and geotechnical data and OSL dating suggest that these faunas occur within Unit 2 which is dated in vibrocore VC3b to 735 ± 134ka. This unit is equivalent to the offshore Yarmouth Roads formation (Cameron *et al.* 1992) and the onshore Cromerian complex.

Within cores VC7c and VC8c1 (except the lowest sample at 36.53mbOD) the foraminifera are indicative of more "modern" assemblages and the presence of large numbers of *Ammonia beccarii* is indicative of warm stages. Within VC7c the productive samples are clearly indicative of a brackish environment of muddy creeks with an increasing marine influence noted up profile. These samples were from Unit 4 which OSL dating suggests was deposited between 109 ± 11ka and 96 ± 11ka, making it equivalent to the offshore Brown Bank formation. The Seabed Prehistory Great Yarmouth project (Area 254 to the north of area 240) investigated brackish and estuarine deposits (within vibrocore VCGY1 at around 29mbOD) which OSL dating suggests were deposited after 116.7±11.2 ka (Wessex Archaeology 2008). Whilst similar *Cyprideis* and *Ammonia* dominated faunas were recovered, these are not considered indicative of a particular time period but do suggest similar sea level and environmental conditions.

The upper part of vibrocore VC8c1 also contained sediments containing estuarine and brackish faunas which have been dated at 32.00mbOD to 7710–7560 cal BC. And at 31.58mbOD to 6730–6590 cal. BC. These levels are not suitable sea level index points (SLIPs) as the do not lie above bedrock and therefore the effects of autocompaction of the sediment cannot be adequately calculated. It is also noted that many of the foraminifera (the relative abundances of which are often used as the basis of transfer function calculations in order to generate SLIPs) are largely reworked from these levels and that the ostracod faunas are considered more reliable proxies of environmental conditions at these dated levels. The sample at 32.00mbOD contained *Phragmites* reeds with ostracods indicative of a saltmarsh fringing an estuary which is likely to have developed within the tidal frame. The increasing marine influence is noted up profile with the sample at 31.59mbOD being likely to have been deposited in the littoral zone on the edges of an outer estuarine/shallow marine environment. These dates and environmental interpretations, when compared to calculated Holocene sea levels for the period fit Holocene sea level rise (Jelgersma 1979, Shennan and Horton 2002).

Acknowledgements

Thanks to Chris Stevens and Sarah Wyles for identifying plant and molluscan material which occurred within the samples.

References

Athersuch, J., Horne, D.J., and Whittaker, J.E., 1989. Marine and Brackish Water Ostracods. Synopses of the British Fauna (New Series), No.43, 343pp

Boomer, I., 2001. Environmental Applications of Marine and Freshwater Ostracods. In :Haslett, S. K., ed. 2001. Quaternary Environmental Micropalaeontology

Cameron, T.D.J., Crosby, A. Balson, P.S., Jeffery, D.H., Lott, G.K., Bulat, J. and Harrison, D.J., 1992. *The geology of the Southern North Sea*. British Geological Survey, United Kingdom Offshore Report, London HMSO.

Funnell, B. M., 1989. Quaternary, In : Jenkins, D. G. and Murray, J. W. Eds., Stratigraphical atlas of fossil foraminifera. London: Ellis Horwood Ltd., 563-569.

Jelgersma, S., 1979. 'Sea-level changes in the North Sea Basin', in Oele, E., Schüttenhelm, R.T.E. and Wiggers, A.J. (eds.), The Quaternary History of the North Sea, Acta Univeritatis Upsaliensis: Symposium Universitatis Upsaliensis Annum Quingentesimum Celebrantis 2.

Kilyeni T.I., 1972. Transient and genetic polymorphism as an explanation of variable noding on the ostracode Cyprideis torosa. Micropalaeontology. 18. 47-63

Meisch, C., 2000. Freshwater Ostracoda of Western and Central Europe. In: J. Schwoerbel and P. Zwick, editors: Suesswasserfauna von Mitteleuropa 8/3. Spektrum Akademischer Verlag, Heidelberg, Berlin. 522pp

Murray, J.W., 1979, British Nearshore Foraminiferids, Academic Press, London.

Murray, J.W., 1991, Ecology and Palaeoecology of Benthic Foraminifera, 397pp, Longman Scientific.

Shennan, I. and Horton, B., 2002. Holocene land- and sea-level changes in Great Britain.', Journal of Quaternary Science., 17 (5-6). pp. 511-526

Wessex Archaeology, 2008. Seabed Prehistory: Gauging the Effects of Marine Aggregate Dredging. Final Report. Volume IV Great Yarmouth. Unpublished report 57422.34, Wessex Archaeology, Salisbury.

Whittaker, J.E., and Horne, D J., 2009 Pleistocene. In : Whittaker, J.E., and Hart, M.B. (eds), Ostracods in British Stratigraphy. The Micropalaeontological Society, Special Publications. The Geological Society, London, 447-467.

Plant remains / mbOD	33.8	33.24	33	32.7	32	31	29.7	29.1	28.3
Charcoal	-	-	-	-	x	-	-	-	-
Plants unidentified	x	-	x	x	x	-	-	x	x

Table 1. Abundance of taxa per sample in VC2c

Abundance:
x – 1-9 specimens
xx – 9-50 specimens
xxx – greater than 50 specimens
xxxx – greater than 100 specimens

Ostracods / mbOD	31.9	31.5	30.83	29.75	28.62	28.36	28.3	28.11	27.91	27.72	27.52
Aurila convexa	-	-	-	-	-	-	-	-	-	x	-
Carinocythereis carinata	-	-	-	-	-	-	-	-	-	-	x
Cytheridea littoralis	-	-	-	-	-	-	-	x	-	-	-
Cyprideis torosa noded	-	-	-	-	-	-	x	-	-	-	-
Cyprideis torosa smooth	-	-	-	-	-	x	xxxx	xx	xx	xx	xx
Leptocythere psammophila	-	-	-	-	-	-	-	x	-	xx	-
Leptocythere sp.	-	-	-	-	-	-	-	-	x	-	-
Loxoconcha elliptica	-	-	-	-	-	-	xx	xx	xx	xx	xx
Loxoconcha rhomboidea	-	-	-	-	-	-	-	x	xx	x	xx
Paracytherois flexuosa	-	-	-	-	-	-	-	-	x	-	-
Propontocypris trigonella	-	-	-	-	-	-	x	-	-	-	X
Unidentified	-	-	-	-	-	-	x	-	-	-	-
											-
Foraminfera											
Ammonia beccarii	-	-	-	-	-	x	-	-	-	-	-
Ammonia beccarii var. *aberdoveyensis*	-	-	-	-	-	-	x	x	x	x	X
Ammonia beccarii var. *batavus*	-	-	-	-	-	-	x	-	-	-	X
Ammonia beccarii var. *limnetes*	-	-	-	-	-	-	-	x	x	x	-

Ostracods / mbOD	31.9	31.5	30.83	29.75	28.62	28.36	28.3	28.11	27.91	27.72	27.52
Ammonia beccarii var. *tepida*	-	-	-	-	-	-	-	x	x	x	-
Ammonia/Elphidium	-	-	-	-	-	-	x	-	-	-	-
Elphidium crispum	-	-	-	-	-	-	-	xx	-	-	x
Elphidium earlandii	-	-	-	-	-	-	x	-	-	-	-
Elphidium incertum	-	-	-	-	-	-	-	x	-	-	-
Elphidium sp.	-	-	-	-	-	-	xx	x	-	x	-
Elphidium macellum	-	-	-	-	-	-	-	x	-	x	xx
Elphidium williamsoni	-	-	-	-	-	-	x	-	-	-	-
Haynesina germanica	-	-	-	-	-	-	x	xx	xx	-	xx
Jadammina macrescens	-	-	-	-	-	-	x	xx	x	x	x
Miliolids	-	-	-	-	-	-	x	x	x	xx	xx
Milammina fusca	-	-	-	-	-	-	-	-	-	-	xx
Miliolinella subrotundata	-	-	-	-	-	-	-	-	-	-	x
Nonion depressulus	-	-	-	-	-	-	-	-	-	-	x
Quinqueloculina bicornis var. *angulata*	-	-	-	-	-	-	-	-	x	-	x
Quinqueloculina cliarensis	-	-	-	-	-	-	-	-	-	-	x
Quinqueloculina seminulum	-	-	-	-	-	-	-	-	-	x	-
Rosalina williamsoni	-	-	-	-	-	-	-	-	x	-	x
Rotalids	-	-	-	-	-	-	-	-	-	-	xx
Unidentified	-	-	-	-	-	-	x	-	-	-	x
Molluscs											
Anomia ephippum	-	-	-	-	-	-	-	x	x	x	x
Cerastoderma spp.	-	-	-	-	-	-	xx	xx	xx	x	x
Hydrobia	-	-	-	-	-	-	xx	xx	xx	xx	xx
Mytilus edulis	-	-	-	-	-	-	-	x	x	x	x
Ostrea edulis	-	-	-	-	-	-	x	x	x	x	x
Patella/Diodora spp.	-	-	-	-	-	-	-	x	x	x	x
Rissoids	-	-	-	-	-	-	-	x	x	x	xx
Scallop (*Chlamys* type)	-	-	-	-	-	-	-	-	x	x	x
Tellin/Scrobicularia	-	-	-	-	-	-	-	x	x	xx	xx
Broken	-	-	-	-	-	x	-	-	x	-	-
Unidentified	-	-	-	-	-	-	-	-	-	-	-

Ostracods / mbOD	31.9	31.5	30.83	29.75	28.62	28.36	28.3	28.11	27.91	27.72	27.52
Animal remains											
Calcareous tubes	-								xx		x
Crustacean claw	-	-	-	-	-	-	x	-	-	-	x
Echinoid pieces	-	-	-	-	-	-	-	x	-	xx	x
Sponge spicules	-	-	-	-	-	-	x	-	-	xx	-
Plant remains											
Plants unidentified	-	-	-	-	x	xx	xx	x	x	-	-
Ruppia spp.	-	-	-	-	-	-	-	x	x	-	-
Wood	-	-	-	-	-	-	x	-	-	-	-

Table 2. Abundance of taxa per sample in VC7c
Abundance:
x – 1-9 specimens
xx – 9-50 specimens
xxx – greater than 50 specimens
xxxx – greater than 100 specimens

Ostracods / mbOD	36.53	35.2	33.65	33.05	32.78	32.52	32.26	32.06	32	31.93	31.81	31.69	31.59
Candona sp.	-	-	-	x	-	-	-	-	-	-	-	-	-
Callistocythere littoralis	-	-	-	-	-	-	-	-	x	-	-	-	-
Cyprideis torosa noded	-	-	-	-	-	-	x	-	-	-	-	-	-
Cyprideis torosa smooth	-	x	-	x	x	xx	xxx	xx	x	x	-	-	x
Cytheropteron sp.	-	-	-	-	-	-	-	-	-	-	-	-	x
Cutherura sp.	-	-	-	-	-	x	-	-	-	-	-	-	-
Cytherura gibba	-	-	-	-	-	-	-	-	-	-	-	-	xx
Elofsonia baltica	-	-	-	-	-	-	-	x	-	-	-	-	x
Elofsonia concilla	-	-	-	-	-	-	-	-	-	-	x	-	-
Hemicythere sp.	-	-	-	-	-	x	-	-	-	-	-	x	x
Hemicythere villosa	-	-	-	-	-	x	-	-	-	-	-	-	-
Heterocythereis albumaculata	-	-	-	-	x	xx	-	x	xx	xx	xx	xx	x
Hirschmannia viridis	-	-	-	-	x	x	-	x	xx	xx	xx	x	xx
Leptocythere sp.	-	-	-	-	-	-	x	xx	x	-	-	-	x
Leptocythere pellucida	-	-	-	-	-	-	-	-	x	x	x	xx	-

Leptocythere psammophila	-	-	-	x	-	-	xx	-	-	-	-	-	-
Loxoconcha elliptica	-	x	-	-	x	xx	xx	xx	x	x	xx	x	xx
Loxoconcha rhomboidea	-	-	-	-	x	x	-	x	xx	-	xx	x	-
Nannocythere sp.	-	-	-	-	-	-	-	x	-	-	-	-	-
Palmoconcha laevata	-	-	-	-	-	-	-	-	-	-	x	-	-
Paracytheridea cuneiformis	-	-	-	-	-	-	-	-	-	x	x	-	-
Pontocythere elongata	-	-	-	-	-	-	-	-	-	-	x	-	-
Propontocypris sp.	-	-	-	-	-	x	x	-	x	x	-	x	x
Propontocypris trigonella	-	-	-	-	-	-	-	x	-	-	x	-	-
Sahnicythere sp.	-	-	-	-	-	-	-	-	-	-	-	-	xx
Semicytherura sp.	-	-	-	-	x	-	-	-	-	-	-	-	-
Semicytherura striata	-	-	-	-	-	-	-	-	-	x	x	x	-
Broken	-	-	-	-	-	-	x	x	-	-	-	x	-
Unidentified	-	-	-	-	-	-	x	xx	-	x	-	x	-
Foraminfera													
Ammonia beccarii	-	x											
Ammonia beccarii var. *aberdoveyensis*	-	x	-	xx	xx	xx	x	x	xx	xx	xx	xx	xx
Ammonia beccarii var. *batavus*	-	-	-	x	xxx	xxx	xx	xx	x	xx	x	xxx	xxx
Ammonia beccarii var. *limnetes*	-	x	x	xxx	xx	xx	x	x	xx	xx	xx	xx	xxx
Ammonia beccarii var. *tepida*	-	x	-	xx	xx	xx	x	x	xx	xx	xx	xx	xxx
Ammonia/Elphidium	-	x	-	-	-	-	-	-	-	-	-	-	-
Astergerinata mammilla	-	-	-	-	-	-	-	-	-	-	x	-	-
Brizalina sp.	-	-	-	-	-	-	-	-	x	-	-	-	-
Brizalina variabilis	-	-	-	-	-	-	-	-	-	x	-	x	x
Cibicides lobatulatus	-	-	-	-	-	-	-	-	-	-	-	x	-
Elphidiella sp.	x	-	-	x	-	-	-	-	-	-	-	-	-
Elphidium crispum	-	-	-	-	-	-	-	x	x	-	-	xx	-
Elphidium gerthi	-	-	-	-	x	x	-	x	x	xx	x	x	-
Elphidium sp.	-	-	-	-	-	-	-	-	x	-	-	x	xx
Elphidium incertum	-	-	-	x	-	-	-	x	x	-	-	x	xx
Elphidium macellum	-	-	-	-	-	-	-	x	xx	xx	xx	xx	x
Elphidium williamsoni	-	-	-	-	x	-	-	-	-	-	-	x	xx
Haynesina germanica	-	-	-	x	xx	xx	-	x	xx	x	-	xx	xx

Jadammina macrescens	-	-	-	x	-	-	x	x	-	-	-	-	x
Lagena sp.	-	-	-	-	-	-	-	-	-	-	x	x	-
Lagena semistriata	-	-	-	-	-	-	-	-	-	-	-	x	-
Lamarckina haliotidea	-	-	-	-	-	-	-	-	-	x	x	x	-
Massilina secans	-	-	-	-	-	x	-	-	-	-	-	x	-
Miliolids	-	x	-	xx	xx	xx	xx	xx	xx	x	x	xxx	xx
Miliolinella subrotundata	-	-	-	-	x	x	x	x	x	x	x	xxx	-
Nonion depressulus	-	-	-	-	-	-	-	-	x	xx	-	x	-
Planorbulina mediterranensis	-	-	-	-	-	-	-	-	x	-	-	-	-
Protelphidium orbiculare	x	-	-	-	-	-	-	-	-	-	-	-	-
Quinqueloculina bicornis	-	-	-	-	-	-	x	-	-	-	-	-	-
Quinqueloculina bicornis var. *angulata*	-	-	-	x	x	x	-	-	-	-	-	-	xx
Quinqueloculina cliarensis	-	-	-	x	-	-	x	x	x	x	x	x	-
Quinqueloculina dimidiata	-	-	-	-	x	x	-	x	x	x	-	x	-
Quinqueloculina lata	-	-	-	-	-	x	-	-	-	-	-	-	-
Quinqueloculina seminulum	-	-	-	-	-	x	-	x	x	-	x	x	-
Quinqueloculina sp.	-	-	-	-	-	xx	-	-	-	-	-	-	-
Quinqueloculina subrotundata	-	-	-	-	-	-	-	-	-	-	-	-	xx
Rotalids	-	-	x	-	-	x	-	xx	-	-	-	-	-
Spirillina vivpara	-	-	-	-	-	-	-	-	x	-	-	-	-
Molluscs													
Bithynia spp.	-	-	-	x	x	x	xx	-	-	-	-	-	-
Bithynia operculum	-	-	-	-	xx	xx	-	-	-	-	-	-	-
Bivalves	xx	-	-	-	-	-	-	x	-	x	xx	xx	x
Broken shell	-	-	-	-	xx	-	-	-	-	-	-	xx	-
Cerastoderma spp.	x	x	x	x	xx	x	xx	-	-	-	x	-	-
Hydrobia	-	x	-	x	xx	xx	xx	x	-	x	xx	-	-
Mytilus edulis	x	-	-	-	x	x	x	-	-	-	-	-	-
Ostrea edulis	-	-	-	x	xx	x	-	x	-	-	-	-	-
Patella/Diodora spp.	x	-	-	-	-	x	-	-	-	-	-	-	-
Piscidium	-	-	-	-	-	-	x	-	-	-	-	-	-
Planorbids	-	-	-	x	-	-	-	-	-	x	-	-	-
Rissoides	-	-	-	-	x	x	-	-	-	-	-	-	-

Tellina/Scrobicularia type	-	-	-	-	x	x	-	-	-	-	x	-	-
Theodoxius fluviatilis	-	-	-	x	xx	x	xx	-	-	-	-	-	-
Valvata sp.	-	-	-	-	x	x	-	-	-	-	-	-	-
Venerupidae	x	-	-	-	-	-	-	-	-	-	-	-	-
Whelk *Buccinum*	-	-	-	-	x	-	-	-	-	-	-	-	-
Unidentified	-	-	-	-	x	-	-	-	-	-	-	-	-
Animal remains													
Barnacle plates	xx	-	-	x	-	-	-	-	-	-	-	-	-
Calcareous tubes	-	-	-	-	-	x	-	-	-	-	xx	xx	x
Crustacean claw	-	-	-	-	-	x	x	x	-	-	-	-	-
Echinoid pieces	-	-	-	-	-	-	-	x	-	xx	-	-	-
Echinoid spines	xx	-	-	-	-	-	-	x	-	xx	-	-	-
Sponge spicules	-	-	-	-	-	-	xx	x	-	-	-	xx	-
Plant remains													
Charcoal	-	-	-	-	-	-	-	-	-	-	x	-	xx
Charophyte oogonium	-	-	-	x	-	-	-	-	-	-	-	-	-
Diatom	-	-	-	-	-	-	-	x	-	-	-	-	-
Plants unidentified	-	-	-	-	-	-	-	-	-	-	x	xx	-
Seed unidentified	-	-	-	-	-	-	-	-	-	-	-	-	x

Table 3. Abundance of taxa per sample in VC8c1
Abundance:
x – 1-9 specimens
xx – 9-50 specimens
xxx – greater than 50 specimens
xxxx – greater than 100 specimens

Ostracods / mbOD	32.5	32.05	31.9	31.98	31.83	31.8	31.61	30.61	28.75	27.9	27.5
Heterocythereis albomaculata	-	-	-	-	-	x	-	-	-	-	-
Foraminfera											
Ammonia beccarii	x	-	x	x	x	-	-	-	-	-	-
Cibicides lobatulatus	x	-	-	-	-	-	-	-	-	-	-
Elphidiella cf. *hannai*	xx	xx	x	xx	x	-	-	-	-	-	-
*Elphidium*sp.	-	xx	-	-	-	-	-	-	-	-	-
Elphidium cf. *arcticum*	-	x	-	-	-	-	-	-	-	-	-
Elphidium/Elphidiella	x	x	x	x	x	-x	-	-	-	-	-
Lagena sp.	x	-	-	-	-	-	-	-	-	-	-
Lamarckina haliotidea	-	x	-	-	-	-	-	-	-	-	-
Protelphidium orbiculare	xx	-	x	x	x	-	-	-	-	-	-
Rotaliid unidentified	x	x	x	x	x	-	-	-	-	-	-
Uvigerina/Buliminella	x	-	x	-	x	-	-	-	-	-	-
Animal remains											
Barnacle plates	-	x	-	-	-	-	-	-	-	-	-
Plant remains											
Diatom	-	-	-	-	-	-	x	-	-	-	-
Plants unidentified	x	x	-	-	-	x	-	-	-	x	-
Wood	-	-	-	-	-	-	-	x	-	-	-

Table 4. Abundance of taxa per sample in VC9c
Abundance:
x – 1-9 specimens
xx – 9-50 specimens
xxx – greater than 50 specimens
xxxx – greater than 100 specimens

WESSEX ARCHAEOLOGY LIMITED.
Registered Head Office: Portway House, Old Sarum Park, Salisbury, Wiltshire SP4 6EB.
Tel: 01722 326867 Fax: 01722 337562 info@wessexarch.co.uk
Regional offices in **Edinburgh**, **Rochester** and **Sheffield**
For more information visit **www.wessexarch.co.uk**